CHAPTER V

Ambiguity Removal and Assimilation of Scatterometer Data*

Abstract. The ERS-1 scatterometer has proved to be a source of high quality ocean surface wind data, but a problem remains, namely the dual directional ambiguity of the solutions. An ambiguity removal scheme, called PRESCAT, is described based on our experience (a) that information on wind direction retrieval skill is an important input to ambiguity removal, (b) that wind-vector filtering is beneficial compared to wind-direction filtering, and (c) that meteorological forecast information already enables us to correctly remove 95% of all ambiguities. The performance of the ambiguity filter is very good compared to other operational ambiguity removal schemes. Furthermore, a statistical interpolation analysis system called 'buddy' check is used effectively to identify and remove the few (approx. 0.1%) wrongly selected solutions.

Assimilation of scatterometer winds has a beneficial impact on analyses and short-range forecasts, probably mainly from improvements on the sub-synoptic scales. On the wider temporal and spatial scales, scatterometer winds were also found beneficial, but only in the absence of satellite temperature soundings (SATEMs). In assimilation experiments in which the latter were included, the scatterometer provided a neutral impact on the medium-range forecast. Moreover, the conventional observations, including SATEMs, are shown to have adverse effects on the surface-wind analysis. We believe that both the redundancy and the adverse effects on the surface-wind field are explained by the rigid formulation of the 6-hour-forecast error structure; the forecast error is assumed flow-independent, and information on the special meteorological conditions in the atmospheric planetary boundary layer is lacking. To make observational systems more useful and complementary for numerical weather prediction the effects of the structure functions have to be investigated more precisely. In an adaptive four-dimensional variational assimilation scheme the effect of the assumptions on forecast-error structure will be less. We show that, in a variational framework, scatterometer backscatter measurements are difficult to assimilate directly. Instead, we derive and illustrate an alternative procedure to assimilate retrieved winds rather than backscatter measurements.

---

*Based on:

Stoffelen, Ad, and David Anderson, Ambiguity Removal and Assimilation of Scatterometer Data, *Q. J. R. Meteorol. Soc.*, 123, 491-518, 1997.

1. Introduction

The European Space Agency's remote-sensing satellite, ERS-1, was launched on 17 July 1991, carrying a C-band scatterometer. The satellite flies in a polar orbit at a height of 800 km. The scatterometer instrument (which is also mounted on ERS-2) has three independent antennae pointing in a horizontal plane towards a direction of 45°, 90°, and 135° with respect to the satellite propagation, thus illuminating a site in the scatterometer's swath three times, by the fore, mid, and aft beam, respectively. The incidence angle of the radar beam varies from 18° to 47° for the mid beam, and from 24° to 57° for the fore and aft beams. The swath, approximately 500 km wide, is sampled every 25 km resulting in 19 measurement nodes across the swath; along the swath the sampling distance is also equal to 25 km. The nodes are not independent, however, and the effective spatial resolution of the instrument on the earth's surface (called the footprint) is approximately 50 km. At the European Centre for Medium-range Weather Forecasts (ECMWF) a quality control procedure has been implemented which can identify and reject anomalous triplets of backscatter measurements [*Stoffelen and Anderson*, 1995; Chapter II]. It was also shown that the scatterometer data can successfully be interpreted as measurements of the 10-m wind vector. Through comparison with the ECMWF numerical weather-prediction (NWP) model, scatterometer winds are found to be more accurate than conventional ocean surface wind data, currently used in operational meteorology [*Stoffelen and Anderson*, 1995; Chapter IV]. However, scatterometer winds have a dual ambiguity because there are two wind solutions at each node on the earth's surface. Several ambiguity removal schemes were evaluated before the launch of ERS-1 [*Graham et al*., 1989], and a scheme called CREO [*Cavanié and Lecomte*, 1987] was selected and implemented by the European Space Agency (ESA). In this scheme two antiparallel fields from the two solutions at each node are built up. For each field the number of cases in which the highest probability solution is chosen is calculated. When this number is significantly higher for one of the fields than for the other, then the field with the higher number is selected. This application of CREO is called 'autonomous' ambiguity removal. If autonomous ambiguity removal fails, or is not applied, then a comparison is made between both antiparallel fields and a forecast of the surface wind field; the field with the higher correlation selected. In section 2 we briefly discuss the performance of this scheme when used with real data, and propose an alternative scheme, based on the United Kingdom Meteorological Office (UKMO) scheme SLICE [*Offiler*, 1987], which improves the ambiguity removal skill.

Given the high quality of the retrieved scatterometer winds, it is important that they be assimilated into numerical weather-prediction (NWP) models. Earlier assimilation experiments with SEASAT scatterometer data in the T106 spectral resolution ECMWF model had a neutral impact in both southern and northern hemispheres [*Anderson et al*.,

1991]. In the case of the rapidly developing QE-2 storm, the KNMI (Koninklijk Nederlands Meteorologisch Instituut) limited area model (LAM) gave a forecast that was better than the ECMWF model's forecast [*Stoffelen and Cats*, 1991], and the use of SEASAT scatterometer data had a further substantial and beneficial effect on the forecast. Preliminary tests with ERS-1 scatterometer data in the ECMWF T106 model showed a neutral impact [*Hoffman*, 1993]. However, the quality of the SEASAT and the preliminary ERS-1 scatterometer data used by Hoffman is substantially less than the current quality of the ERS-1 scatterometer data. Assimilation experiments at the UK Meteorological Office showed that the ERS-1 scatterometer winds had a beneficial impact in a day-5 forecast in the southern hemisphere [*Bell*, 1994]. *Breivik et al.* [1993] obtained a small beneficial effect in the Norwegian 50-km resolution limited-area model.

For many years, ECMWF have been using a statistical interpolation scheme, otherwise known as optimal interpolation or OI, to perform the analysis. To test whether the data can be used to modify the ECMWF analyses using the current OI analysis scheme, various experiments are done in which winds from the ERS scatterometer processing, inversion, and ambiguity removal scheme, called PRESCAT, are assimilated into the ECMWF model analysis. One of the periods selected is from 18 to 28 March; it is chosen so as to coincide with a parallel study being conducted by the UK Meteorological Office [*Bell*, 1994].

Parallel assimilation experiments to assess the 'redundancy' between surface wind data and NOAA/NESDIS (National Oceanographic and Atmospheric Administration/National Environmental Satellite and Data Information System) processed TOVS (TIROS (Television Infra-Red Operational Satellite) Operational Vertical Sounder) vertical temperature soundings [*Smith et al.*, 1979], called SATEM, are also discussed in section 3. Ten-day forecasts from these assimilations were made and are compared with the verifying analyses to test for impact of the scatterometer data on the forecast. Since scatterometer data had not yet been used operationally at ECMWF, they can therefore be used to verify the operational ECMWF surface wind analyses and forecasts, as is demonstrated in section 3.4.

In recent years variational assimilation schemes have become more mature, and at ECMWF a scheme of this kind has been developed but, at the time of writing, has not yet been implemented [*Courtier et al.*, 1993]. It was anticipated that satellite measurements that are indirectly related to NWP model variables, are best assimilated *directly* into such schemes. In section 4, however, it is shown that this is not the case for scatterometer measurements, and that it is more practicable to assimilate the ambiguous winds rather than the scatterometer backscatter measurement values s^0. The paper ends with a summary and conclusions in section 5.

2. Ambiguity Removal

We found that a modified application of CREO at ECMWF worked fairly well in about 65% of cases, but in a relatively large number of cases (approx. 30%) CREO did not provide a solution even when reasonable retrieved winds were present. In a small number of cases (approx. 5%) the solution provided by CREO was wrong. These cases tended to be associated with rapidly changing and/or complex synoptic situations, for which correct scatterometer winds would have been especially valuable. *Stoffelen and Anderson* [1995; Chapter II] have shown that the probability of the two wind-vector solutions is close to 50% and that the rank of the correct solution is horizontally correlated, which implies that autonomous ambiguity removal is not likely to be very successful; a conclusion that indeed was found to be true. Consequently we developed a procedure to use a short-range forecast to select direction at every node, and introduced a revised ambiguity removal procedure within the PRESCAT package.

2.1. Description of the Ambiguity Removal Procedure

First a selection of direction is made by choosing that retrieved solution whose direction is closest to the background wind field. This selection is made from the two solutions provided by the previous inversion step [*Stoffelen and Anderson*, 1995; Chapter II]. Experience has shown that the field so produced is reasonable most of the time but there are local regions, i.e., in about 5% of cases, where the solution appears unmeteorological. It is therefore advisable to apply a filter in an attempt to increase meteorological consistency. The choice of selection filter used here was influenced by SLICE [*Offiler*, 1987], but it differs from SLICE in a number of ways, as is discussed below.

The filter consists of a 5×5 box which slides over the wind field, up to 114 rows at a time. The box first slides in the direction opposite to that of the satellite, starting at the inside edge of the swath and proceeding as in Figure 1a. When it reaches the end of the sector, the direction is reversed, and it exactly retraces its track. On the third pass it starts at the outside edge of the swath and proceeds as in Figure 1b. On the fourth pass it exactly reverses the trace of the third pass. In SLICE the scheme finishes processing when there are less than a certain number of points changed in a pass. However, it was found that even if there were no changes made on one pass there could be changes on the next pass, and that these changes were, in general, beneficial. In PRESCAT there are always four passes.

Within a 5×5 box, the direction at the center of the box is chosen, based on a weighted average of the differences from the N surrounding points, of which there are usually 24; but there may be less near the edge of the swath if part of the box is over land, or, if some points have been rejected by the quality control on the backscatter measurements. At the central point, a mean likelihood, L_i, is calculated for each solution i

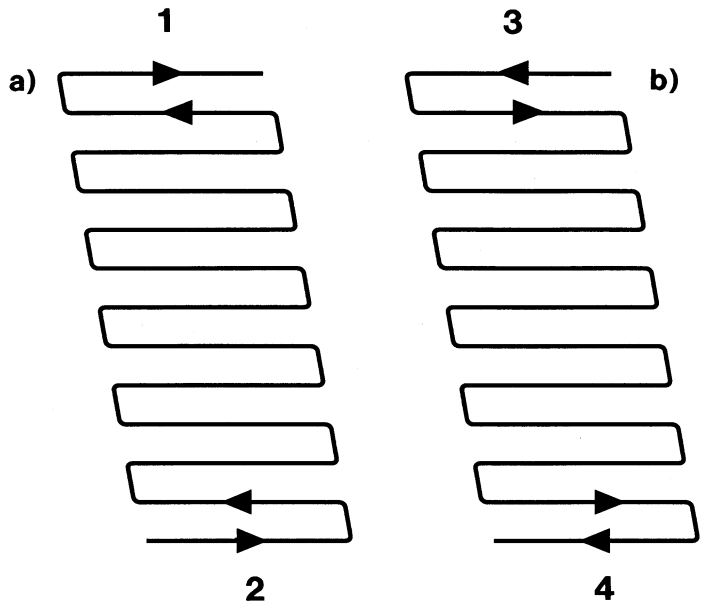

Figure 1. Schematic of the way that the ambiguity removal filter slides along an ascending orbit in (a) the first two iterations and (b) the second two iterations.

where

$$L_i = \frac{\sum_{j=1}^{N} C_j \exp[-0.5\{(u_i - u_j)^2 + (v_i - v_j)^2\}q^{-2}]}{N} \qquad (1)$$

and the summation on j is over the N surrounding points in the box. The solution, i, with the highest probability L_i is then selected. The parameter q^2 should represent the wind component variability within a box. Currently a value of q = 2.5 m s^{-1} is used. When a lower value, 2.0 m s^{-1}, was used, the filter was unable to influence neighboring points sufficiently. In PRESCAT the computed likelihood of a solution depends on the wind vector (Eq. (1)) rather than just direction as in SLICE, since we found several cases (near fronts) where speed as much as direction indicated the consistency between neighboring points.

The parameter C_j represents the confidence in the solution at node j. The initial value of C is

$$C = \frac{P \times A \times NN}{4} \qquad (2)$$

where P is the scaled probability that the wind direction is within, say, 5° of the true direction, A is the probability that the current solution is the correct one, and NN is the number of nearest neighbors. A quantity I indicates the skill with which wind direction can be resolved from the radar back-scatter measurements. P is derived from I, which in turn is defined in Eq. (4.4) of *Stoffelen and Anderson* [1995; Chapter II]. As I can range from zero to quite high values for high speeds and outer nodes, it is necessary to map it to the range 0 to 1 so as to use it as a probability index of skill. The mapping $P = I'(2 - I')$ where I' =

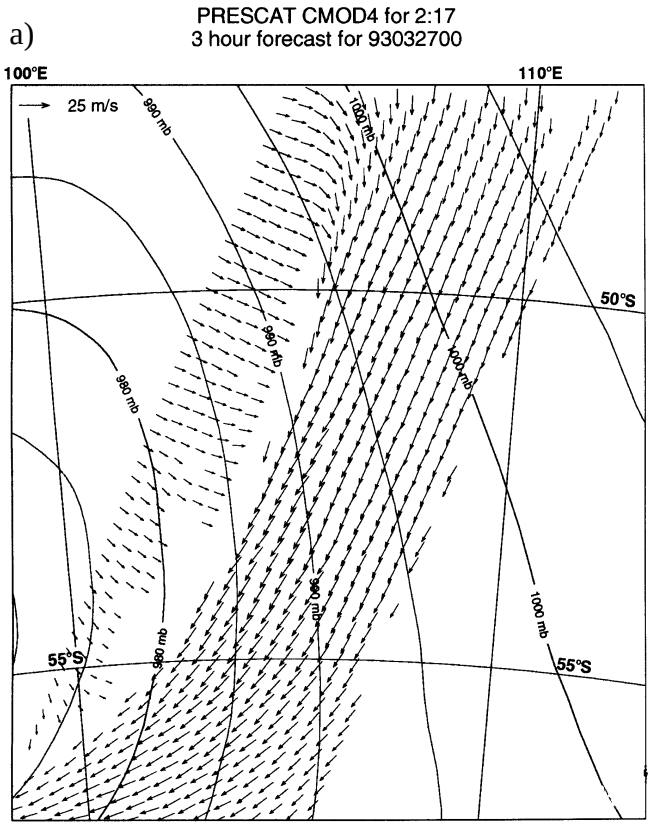

Figure 2. (a) Winds retrieved and with ambiguities removed by PRESCAT for 02 UTC 27 March 1993. Contours are ECMWF 6-hour forecast of mean-sea-level pressure, verifying at 00 UTC. On the right page, (b) FGAT winds, and, (c) winds with ambiguities removed by CREO. In (a) winds with a low confidence rating have not been plotted. These lie mainly along the line of the front, which is very sharp in (a) and (c), but much less so in FGAT. In (c) the winds in area A are in error.

$\min(I/\sqrt{10}, 1)$, has the property of being 0 for I = 0, increasing monotonically with increasing I to a value of 1 at $I = \sqrt{10}$, and is constant when $I > \sqrt{10}$. In the report by *Stoffelen and Anderson* [1995; Chapter II] it was determined empirically that adequate directional skill exists when $I > \sqrt{10}$, as is reflected in the above mapping. The quantity A is defined by the equation

$$A = \exp[-0.5\{(u - u_B)^2 + (v - v_B)^2\}q^{-2}]$$

where A determines the probability that the selected solution is the correct one, and (u, v) is the closest of the two scatterometer wind vectors to the ECMWF model first guess denoted (u_B, v_B). We used FGAT (First Guess at Appropriate Time), where the first guess is interpolated to the measurement time from a 3-, 6-, and 9- hour forecast. The factor *NN* is the number of nearest neighbors to the node under consideration and therefore has a value between 1 and 4. In Eq. (1) points for which C is low are given low weight, and will not have a strong influence on the selection of a solution at neighboring points; the opposite is true for points for which $C \approx 1$. Thus, the filter propagates information with high confidence to areas where confidence is low.

The confidence of a point is updated on a pass of the filter according to

$$C = C + (1 - C)L$$

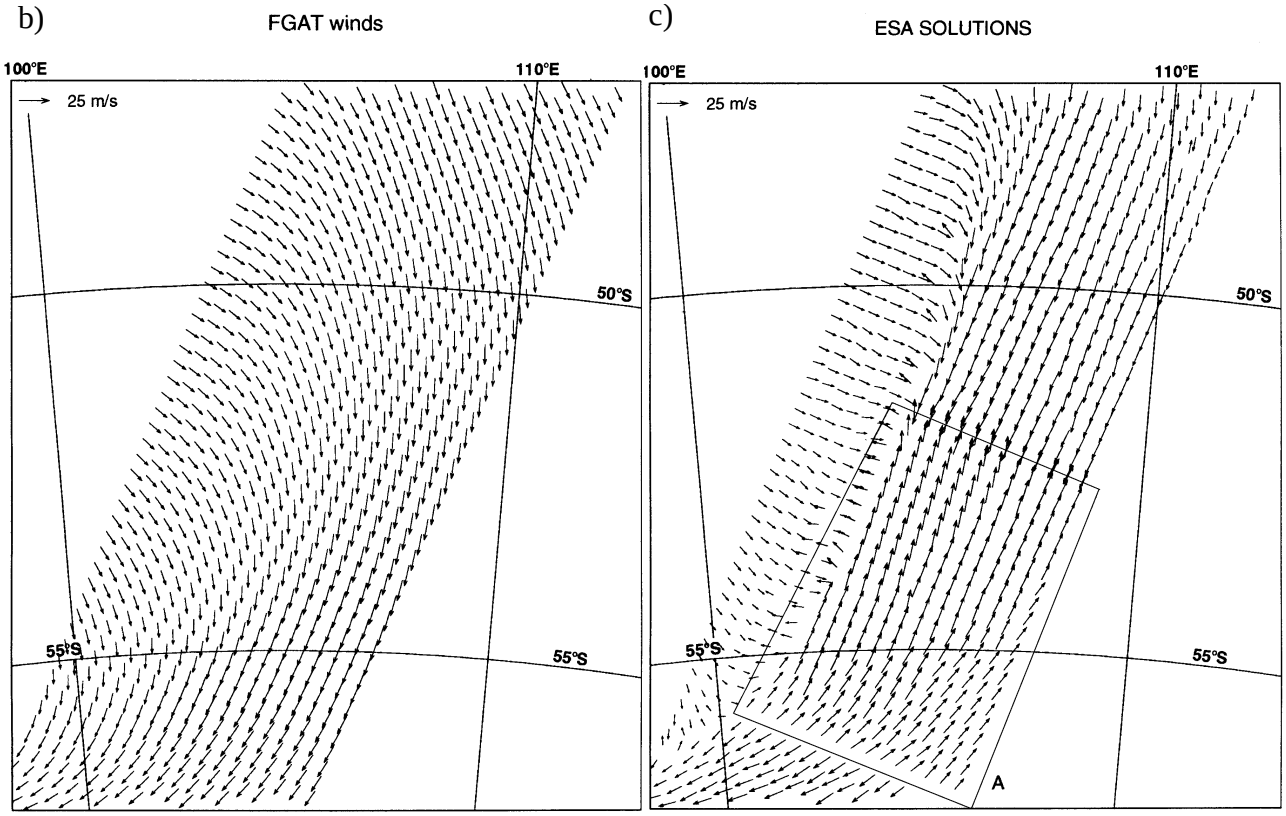

where L is defined in Eq. (1), i.e., confidence is increased relatively mostly when the wind vector at the neighboring points is consistent, and when we have confidence in the neighboring solutions (see, e.g., Eq. (1)). *Stoffelen and Anderson* [1995; Chapter II] have given the description of a consistency check of the three radar measurements at each location whereby anomalous triplets are rejected (1–2%); these are usually in areas with high variability (i.e., fronts, cyclones, etc.). Because the background information is usually also of lower quality in such areas, and because rejection is often associated with wind shifts, the quality control (QC) benefits the ambiguity removal.

In the next section we give a few examples of PRESCAT to both show its power and also highlight some remaining problems. The examples that have been chosen emphasize important meteorological situations.

2.2. Examples of Ambiguity Removal Using PRESCAT

Figure 2a shows a plot of the winds for 02 UTC 27 March 1993 resulting from retrieval and ambiguity removal using PRESCAT. The appropriate FGAT field used in PRESCAT is shown in Figure 2b. The blank areas in the swath in Figure 2a are regions in which data have been rejected by the QC of the inversion procedure. Of most interest is the region close to the front. This is an area in which the winds change rapidly in space and, by implication, also in time, and our hypothesis is that there will be confused sea-state

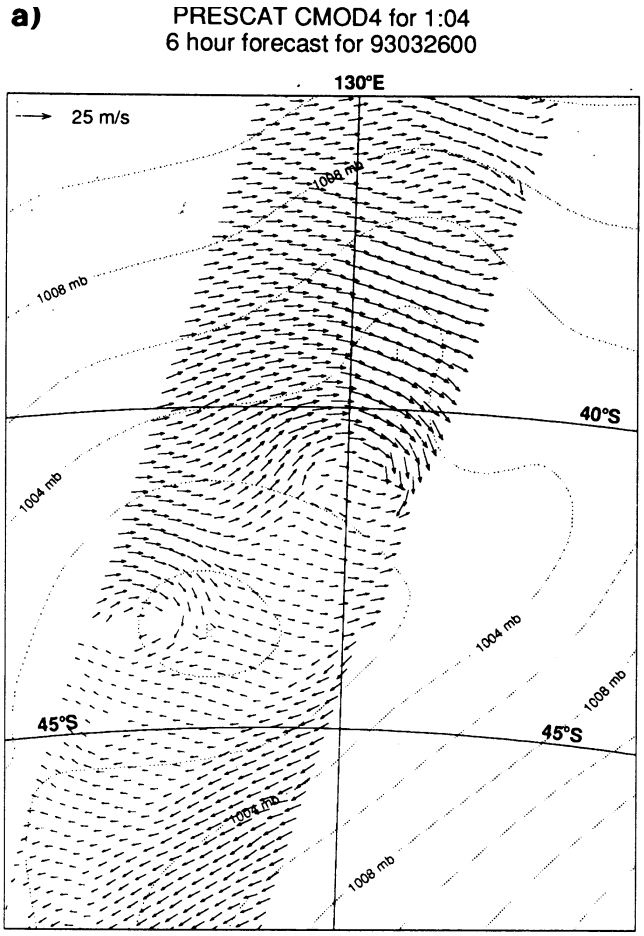

Figure 3. Similar to Figure 2, but for 00 UTC 26 March 1993. This figure shows in panel (a) a complex double low structure in the PRESCAT winds, but in (b), on the right page, FGAT depicts only a broad feature. A shear line is needed somewhere. Its position is unclear, but it should probably join the centers of the two lows. Panel (c) shows the ESA solution. Here, the area marked A is obviously wrong.

conditions. However, in some areas rain may also be a disturbing factor on the sea surface. The QC arises from the s^0 measurements themselves, not from a realization that there is a front. Nevertheless, the front is well delineated by this test.

Figure 2a also shows how well the scatterometer can see sharp features. The front is pinpointed to within 50 km with 90° changes in wind direction across it. By contrast FGAT (Figure 2b) shows a much more gentle turning of the wind and no sharp front. A sharp front is present also in the CREO (ESA) solution (Figure 2c), but in one block of winds the direction is wrongly selected. The origin of this error lies in a wrong selection at the location of the front in the south-west of the area. It is obvious from the observed speed gradient that wind-speed information, as used in Eq. (1), rather than just wind direction information, as used in SLICE, is useful for ambiguity removal.

A second example comprises a complex double-centered low-pressure system which developed in the Australian Bight at 00 UTC 26 March 1993. The PRESCAT solution is shown in Figure 3a. Again a region of high residuals is present in and around the southernmost low-pressure system. These points are towards the outside of the swath where wind direction accuracy is generally highest. This figure is selected to show that complex systems exist where it is hard to choose the correct wind pattern. The chosen pattern (Figure

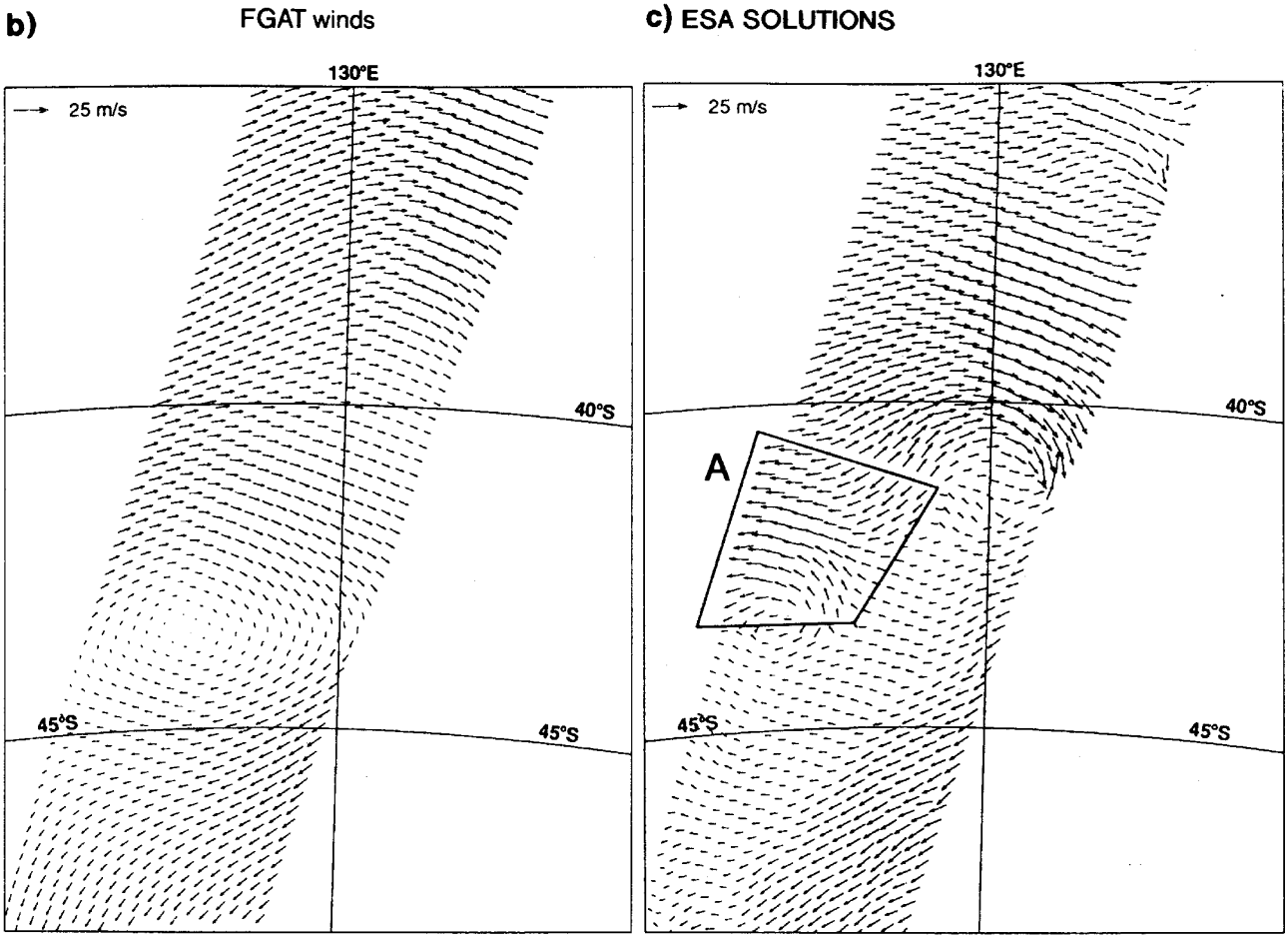

3a) looks unmeteorological in the area east of the southernmost low because there are sharp shear zones with a large shift in direction. A shear line is needed somewhere, probably linking the centers of the two lows, rather than the one selected by PRESCAT. However, in the forecast of surface pressure the southernmost low-pressure system and a wavelike disturbance further to the north-east are present but shifted in position with respect to the scatterometer-measured disturbance.

Part of the difficulty in ambiguity removal arises because the scatterometer can see much smaller-scale features than are present in the FGAT winds (Figure 3b), which shows only a smooth wind field. Finally, Figure 3c shows the CREO solution which is clearly wrong in region A. Errors in PRESCAT can arise when the FGAT directions are roughly along the direction of the wrong solution. In these cases the initially wrongly selected solutions compare relatively well with FGAT and are assigned high confidence (Eq. (2)). If the FGAT is close to 180° wrong for only a few isolated points, then the filter can correct for this. If, however, the area of wrong solutions is large, then the filter is unable to make a satisfactory correction. Errors also arise if the FGAT directions are nearly orthogonal to the pseudo-streamline defined by the scatterometer. (The term pseudo-streamline is used rather than streamline since the rank-1 and rank-2 directions are not exactly antiparallel.) Such

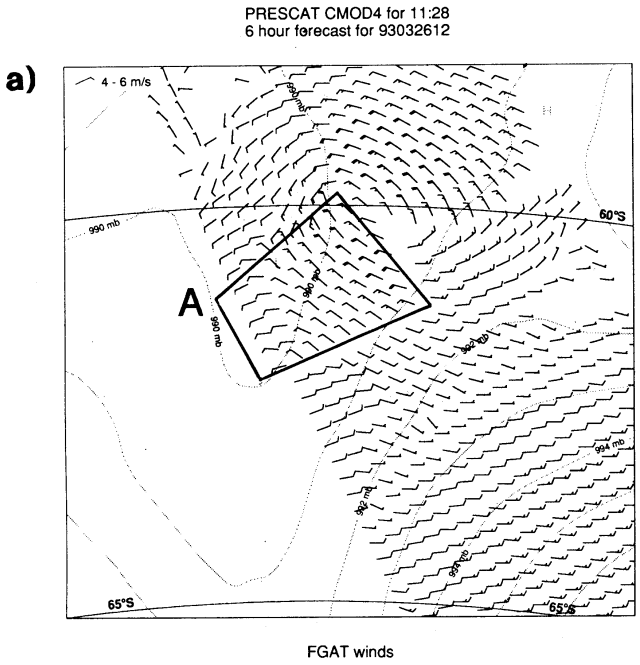

Figure 4. Plots of a low pressure system for 12 UTC 26 March 1993. In (a), ambiguities are removed using the FGAT from the ECMWF operational analysis system shown in (b), while in (c) ambiguities are removed by using FGAT obtained from an experiment in which scatterometer data were assimilated. The latter FGAT was visually close to (b) but just marginally different, leading to improved winds in the sector south-west of the depression. The pseudo streamline is nearly orthogonal to FGAT directions at many nodes in this example. This means that the solutions are very sensitive to small changes in FGAT, and prone to error as in area A in panel (a).

points would be given low confidence and would be corrected by PRESCAT provided they are surrounded by areas of higher confidence. However, if higher confidence areas are not present then errors can occur. The above directional errors can arise when the FGAT winds are light and the wind direction therefore not very important, or when there is a mispositioning of a meteorological system in the first guess. The next two examples provide illustrations.

Figure 4a shows the retrieved winds in an intense polar low at 12 UTC on 26 March 1993, and Figure 4b the corresponding FGAT winds, in which the low is virtually absent. Although PRESCAT has delineated this structure very well in general, there is a patch to the south-west of the depression in which the winds are obviously wrong. The main cause of error in Figure 4a arises because FGAT winds over a significant part of the area are nearly orthogonal to the pseudo-streamline defined by the scatterometer, thus making the direction selected very sensitive to errors in FGAT. There is also a smaller area in which FGAT is closest to the wrong solution. A small difference in FGAT could tip the selected winds by almost 180°, as is illustrated in Figure 4c. In this case FGAT is taken from an experiment in which scatterometer data have been assimilated (see next section). This FGAT is very similar to Figure 4b (not shown), but compares slightly better with the circulation indicated by the scatterometer in the south-west sector of the low. This is just enough to tip the initial selection at a few nodes; subsequently the filter is then able to bring about convergence to the correct solution. This example illustrates the sensitivity that the ambiguity removal has to the quality of the input forecast data. It is also a very good example showing mesoscale features which can be seen by the scatterometer but have not been detected by the ECMWF

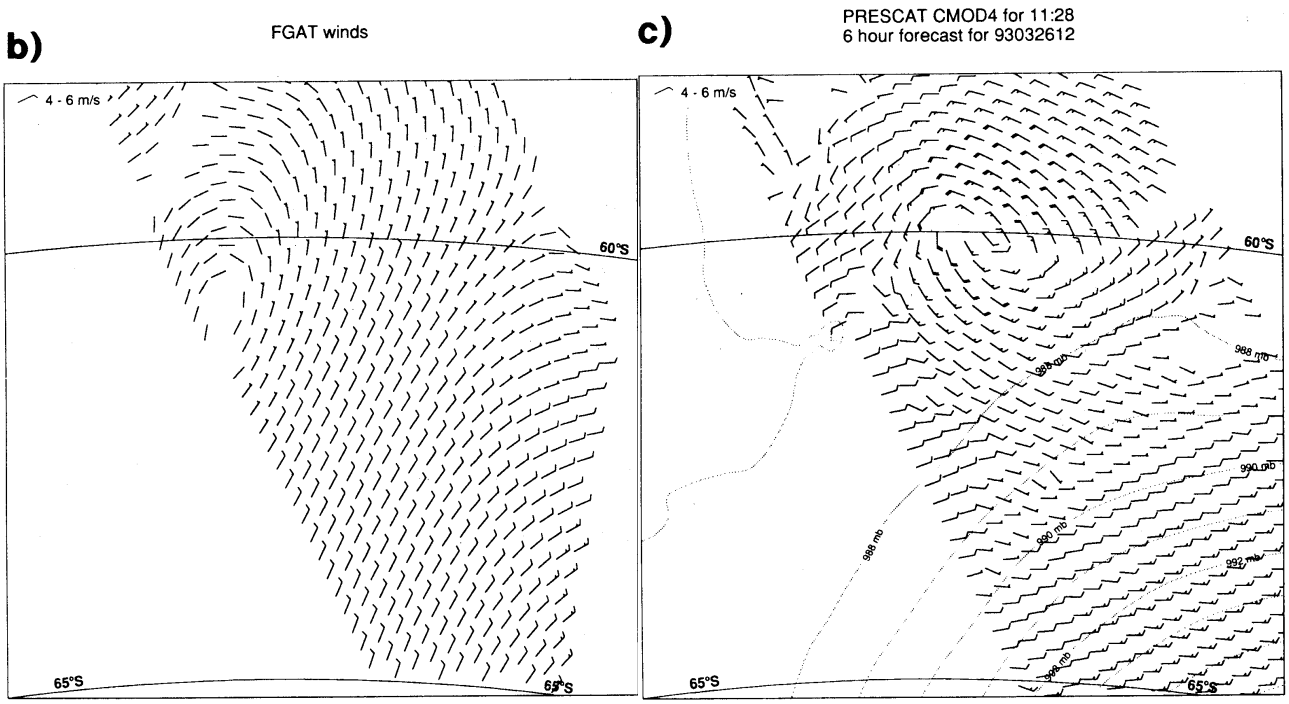

analysis/forecast system, because there were no other useful observations available in this area of the southern hemisphere.

In Figure 5 we show an example of a tropical storm. In this case the FGAT shows a tropical feature with wrong position and weak winds near the center, while the scatterometer shows an active tropical storm. The reason for including this example is two-fold: first to show that PRESCAT can represent tropical storms not present in the FGAT, but secondly there can still be correlated error resulting from large phase errors in FGAT. The batch of winds labeled A is almost certainly in error. In the next section we describe a quality control procedure, called 'buddy' checking, which can effectively remove wrongly selected ambiguities.

When developing PRESCAT, a 6-hour forecast, denoted FG, was used originally as a first guess. However, it was found better to use a first guess which corresponded with the satellite's measurement time (FGAT). For slow moving, large-scale features, this is not necessary, but for rapidly moving systems it is essential. Figure 6 shows the scatterometer winds to the east of a low-pressure system, the deepest ever recorded (which later hit the Shetland islands and the grounded oil tanker Braer in January 1993). In the case for which FG was used rather than FGAT, the winds in the area marked A and B looked unmeteorological and, very likely, were wrong. By using FGAT, and, therefore, a more appropriate comparison between the background winds and the scatterometer winds, a correct wind selection was obtained. Obviously, the use of a forecast with a lead time of between 18 and 36 hours (as is currently done in ESA operations) will degrade the performance of the PRESCAT scheme (or any other scheme using meteorological forecast

information as background for the ambiguity removal procedure).

PRESCAT uses wind-vector consistency in filtering the data. The use of background-error covariance structures to obtain the most likely wind field structure should lead to a meteorologically more consistent analysis and, thus, ambiguity removal. In a variational analysis procedure these structure-functions together with the information provided by the scatterometer can be used to correct errors in the background field. Thus a meteorologically balanced analysis will result, to be used for the benefit of the ambiguity removal. The three-dimensional and four-dimensional variational (3D- and 4D-Var) data assimilation procedures are a sensible framework for further investigation of the variational approach to ambiguity removal (see section 4).

3. Optimum Interpolation (OI) Assimilation

3.1. The Analysis System

The analysis uses a statistical filter, called optimum interpolation (OI) in which the observations and the model forecast are combined into a coherent, balanced analysis. Differences between the model and observations are used to alter the forecast. Although the OI is carried out at discrete 6-hour intervals the correct time of observation (FGAT) is used for the calculation of the difference between observation and model. Data are separated into 6 hour windows.

Since the analysis used is multivariate, measurements of wind will not only influence the wind analysis (as in a univariate scheme where each variable is analyzed separately) but also the mass field (i.e., temperature at a given height or, as in the model, the height of a given pressure surface) through a latitude-dependent application of geostrophy. Near-surface data adjust not only the surface layers but have an influence in the vertical also. Differences between the PRESCAT winds and the FGAT are projected vertically as in Figure 7. This projection is strictly vertical. This is good for mature systems, but probably not so for young developing baroclinic systems.

Since the background error is assumed to have a horizontal structure, the difference between a datum and the FGAT influences an area around the observation with an influence that decreases with increasing distance from the observation. This is defined by the horizontal weighting functions shown in Figure 8. As shown in Section 2, the scatterometer can see mesoscale features very well. In order that we might allow the best possible use of this data in the current analysis system, we used the highest possible model spectral sampling of the ECMWF model, viz. T213, which corresponds to about 60 km spatial sampling, i.e., comparable with the resolution of the scatterometer. However, the effective analysis resolution is likely to be considerably poorer than this, being governed by the

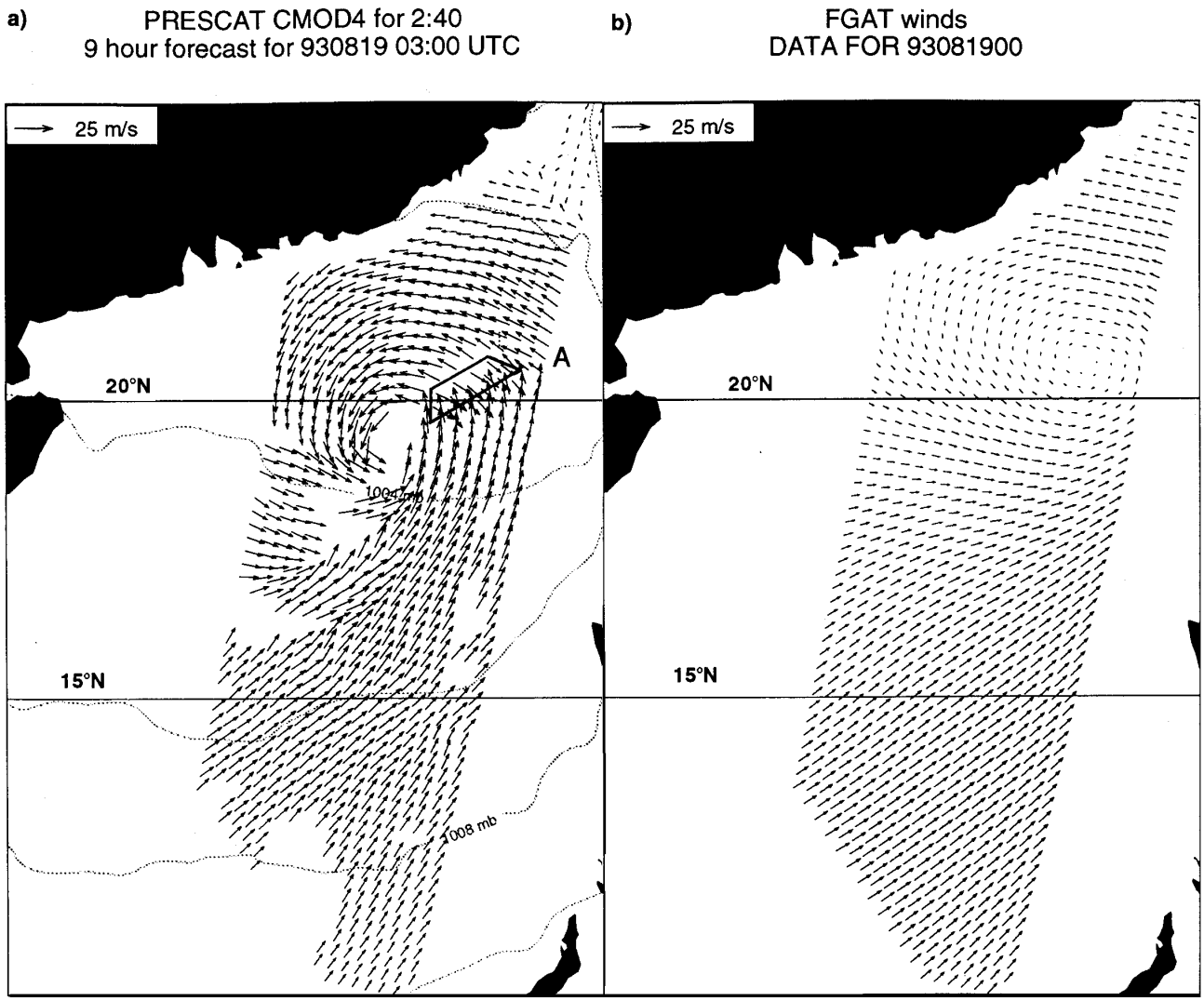

Figure 5. a) Plot of winds with ambiguity removed using PRESCAT. (b) Plot of the FGAT field used in the ambiguity removal. An important tropical cyclone is shown for 19 August 1993. The system is present in (a), but only a weak feature can be seen in (b).

weighting functions shown in Figure 8. Analysis is a costly procedure, so some assimilation experiments were carried out at the reduced model spectral sampling of T106 (approx. 125 km spatial model grid).

Although there are typically 40 000 scatterometer measurements in a 6-hour period, the data presented to the analysis are thinned to 100 km resolution. This is done because the resolution of the analysis is lower than that of the scatterometer and so cannot resolve the structure seen by the scatterometer. To avoid horizontal correlation in the data used for assimilation we performed thinning rather than averaging to achieve 100 km resolution. In retrospect, averaging over 3×3 nodes and thinning to 100 km would have been sufficient, since horizontal wind error correlation is small for scales larger than 50 km [*Stoffelen and Anderson*, 1995; Chapter IV].

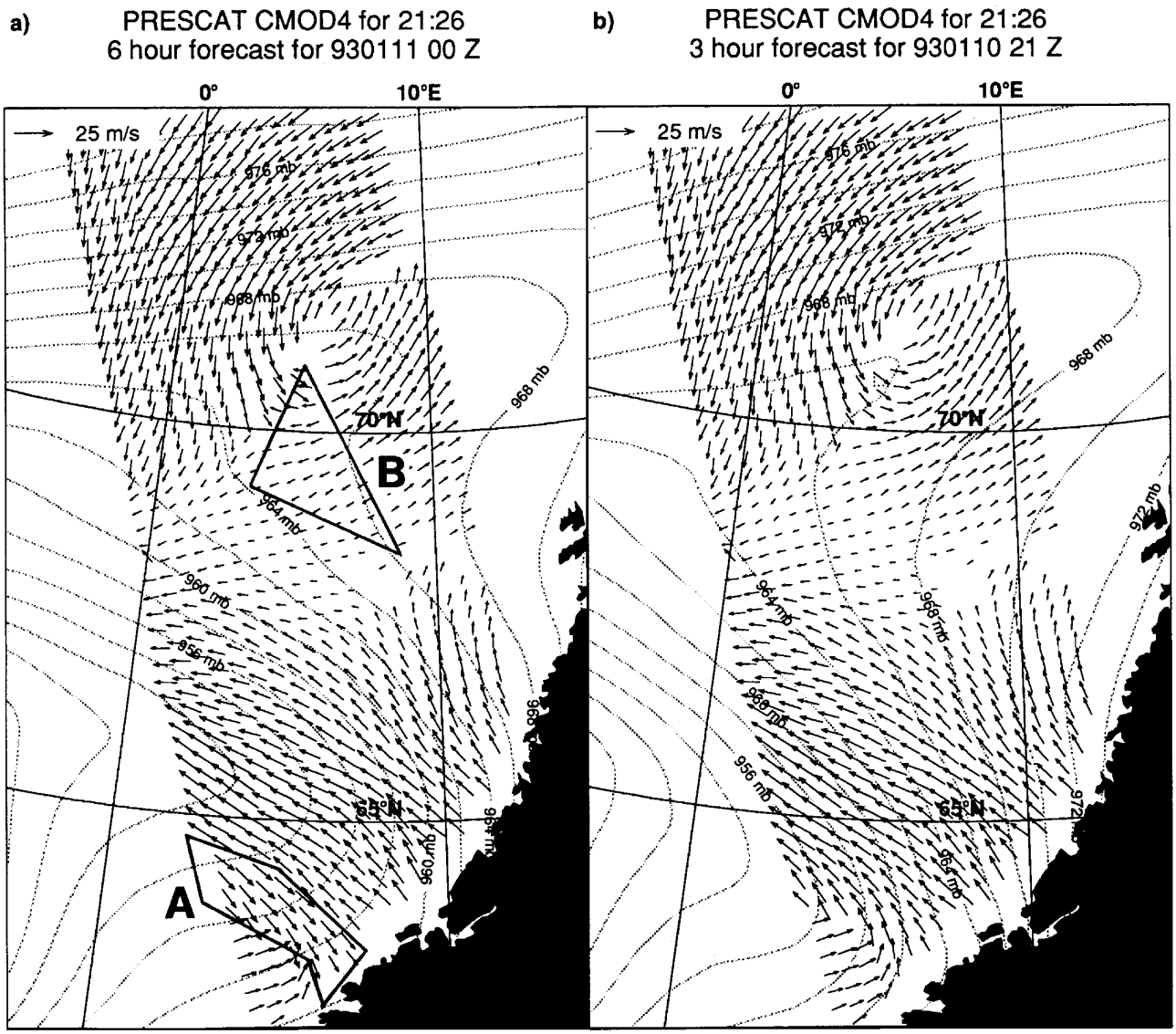

Figure 6. (a) Plot of winds close to the 'storm of the century', with the lowest ever recorded pressure. In this application of PRESCAT, the winds are selected using a forecast valid for the central time (FG), i.e., 00 UTC 12 January 1993. The winds are probably wrong in the areas marked A and B. (b) Winds after ambiguity removal using FGAT at 21 UTC, showing improvement in these areas.

One stage in the analysis procedure consists of a buddy-check. For every datum, an analysis is done without that datum and the value of the analysis is then compared with the measurement. If the difference is large, the datum is rejected. Typically about four PRESCAT winds are rejected every analysis from about 3000 presented to the analysis. Thus, the most serious ambiguity-removal errors are removed.

Table 1. Analysis Experiments

Experiment	Dates (1993)	Grid	Levels	PRESCAT	SATEM/ SATOB
SCAT	18 to 28 March	T213	31	YES	YES
NoSCAT	18 to 28 March	T213	31	NO	YES
SCAT/SATEM	26 April to 1 May	T106	19	YES	YES
NoSCAT/SATEM	26 April to 1 May	T106	19	NO	YES
SCAT/NoSATEM	26 April to 1 May	T106	19	YES	NO
NoSCAT/NoSATEM	26 April to 1 May	T106	19	NO	NO

YES means that the data are assimilated.

3.2. Analysis and Short-Range Impact

Several analysis periods have been considered and forecasts done from these analyses. We consider here only the periods from 12 UTC 18 March 1993 to 12 UTC 28 March 1993 and from 12 UTC 26 April 1993 to 00 UTC 2 May 1993 (see Table 1). Figure 9a shows the differences in the control and assimilated analyses for 12 UTC 18 March, i.e., after a single 6-hour assimilation of scatterometer winds from PRESCAT. Differences in the 1000-mb height are, typically, of order 10 m (approximately 1 mb in surface pressure) although, in the southern hemisphere, larger differences occur of approximately 30 m (i.e., 4 mb). Speed differences at the 10-m level can be up to 10 m s^{-1}. From other experiments, not shown, we found these numbers to be representative. These differences now evolve with time to the next analysis, six hours later, when new data are assimilated and, consequently, changes are made. After a few days of scatterometer data assimilation, differences grow in magnitude and need not be confined to the satellite swath, but in the southern hemisphere cover the storm track belt around Antarctica. However, the differences do not grow indefinitely. Figure 9b shows the differences between the control (NoSCAT) and SCAT assimilation after 10 days of assimilation. Typical differences are a few tens of meters (a few mb) and maximum differences are approximately 140 m, i.e., about 18 mb.

An important question is whether these changes are beneficial. This is not easy to determine. Possible methods of assessment are (a) to compare the fit of the FGAT from the SCAT and NoSCAT runs to the scatterometer data, (b) to compare the fit of other data to the FGAT from the SCAT and NoSCAT runs, or (c) to compare meteorological or wave-model forecasts started from the analyses. The latter approach has been tried using meteorological forecasts (see below) but wave forecasts have not been attempted in this study.

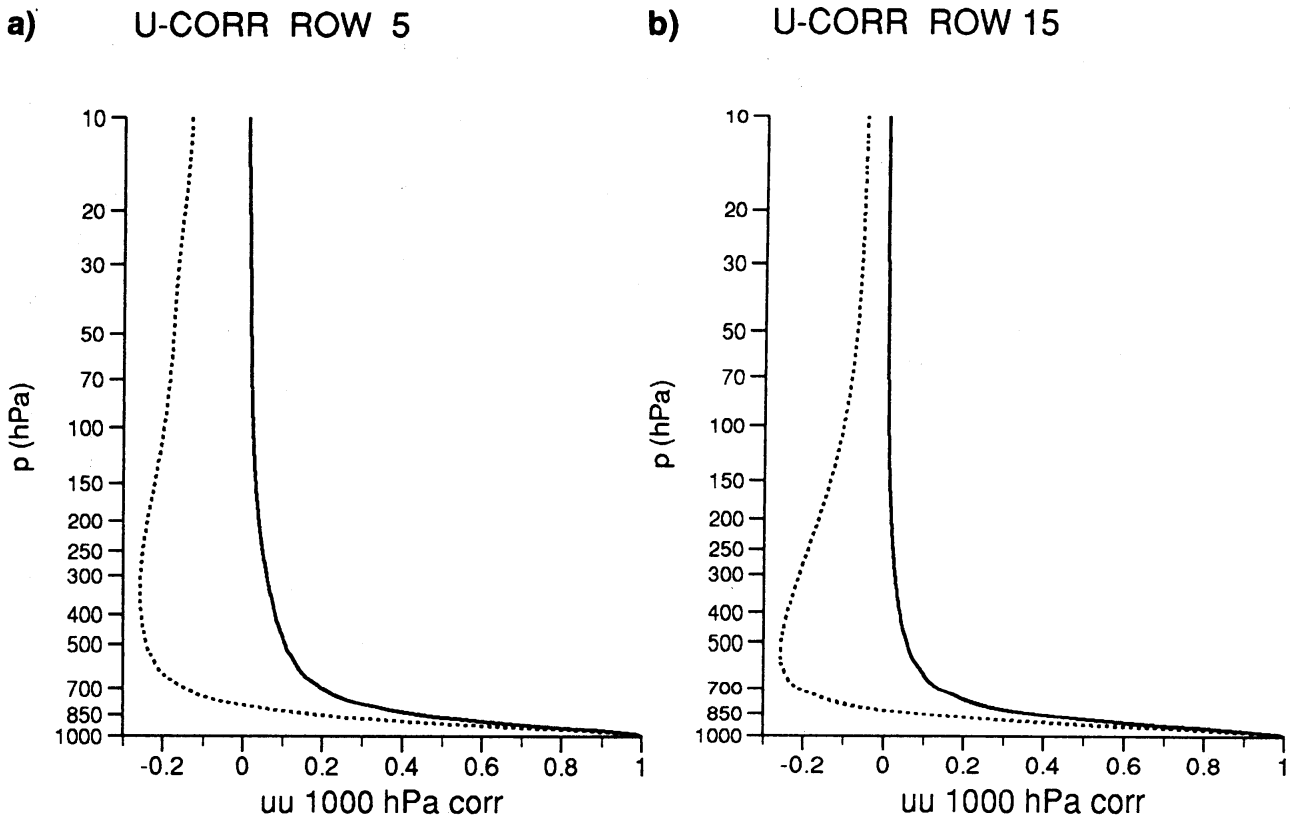

Figure 7. Vertical correlation function in the OI system used to extend surface wind increments in the vertical: (a) mid latitudes; (b) tropics. Continuous line: non-divergent wind component covariance. Dotted line: divergent covariance (from *Undén* [1989]).

As illustrated in Figures 2-5, the synoptic detail possessed by scatterometer data is significantly greater than in the ECMWF model fields and, on a 100 km scale, scatterometer errors are random rather than correlated [*Stoffelen and Anderson*, 1995; Chapters II and IV]. We do expect, therefore, an impact from scatterometer data on the smaller spatial scales and, as a consequence, also on the shorter time scales. To measure the improvement on hese scales in the ECMWF analysis/forecasting system, the same experiments have been verified by direct comparison with observations. In Table 2 we show a comparison between departure statistics of scatterometer minus FGAT winds for the experiment SCAT and the control NoSCAT, averaged over twelve 6-hour windows near the end of the experiment. Vector root-mean-square (RMS) departures are improved by approximately 5%. Because of the polar orbit each location is generally sampled twice a day, therefore passes 6 hours apart are generally well separated geographically and passes 12 hours apart fall in similar geographical areas. The departure statistics are therefore a verification of information from the scatterometer assimilated at least twelve hours earlier.

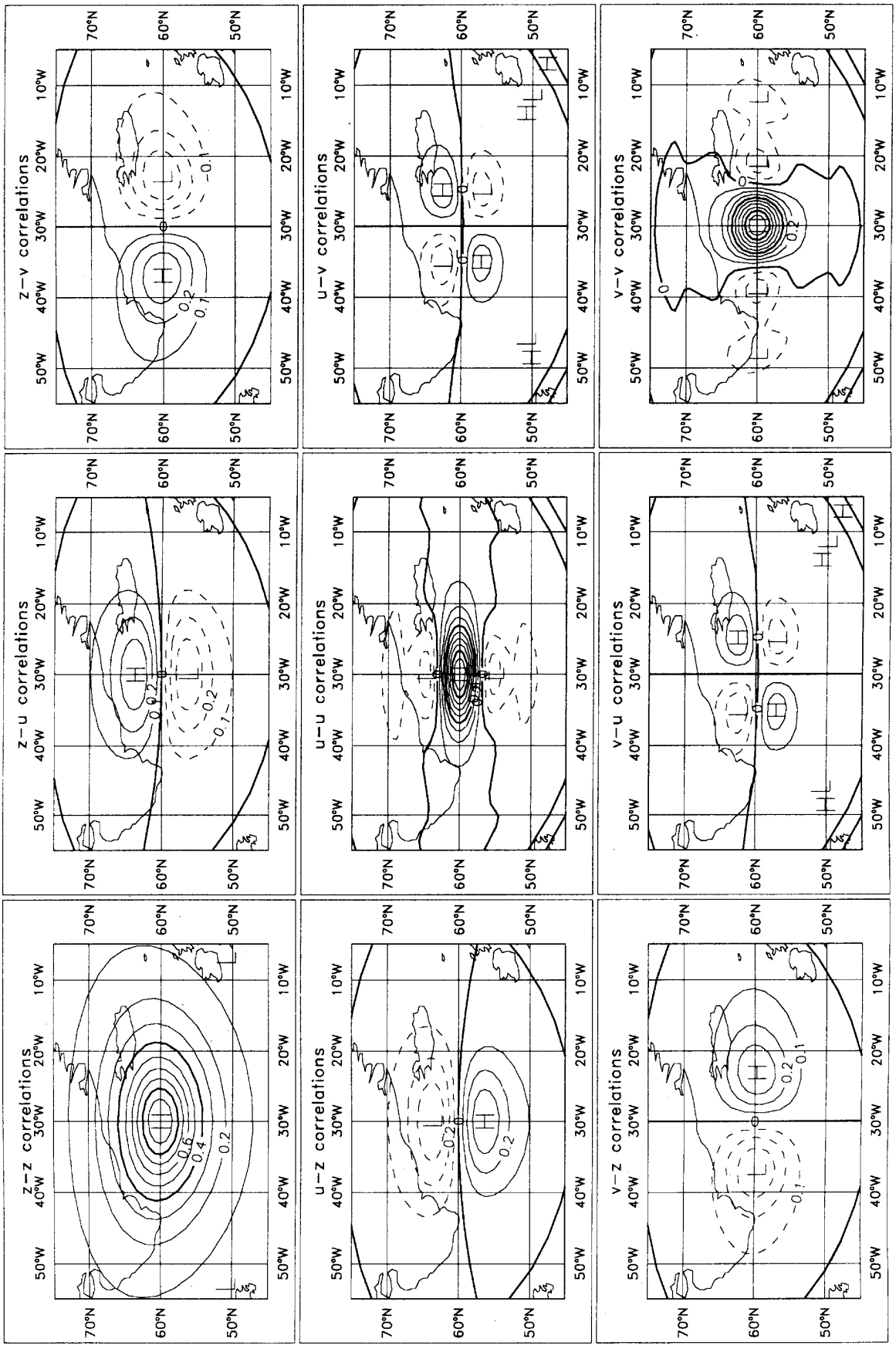

Figure 8. The correlation function used to extend forecast error in the horizontal. From the ECMWF Research manual 1: Data Assimilation, *P. Lönnberg and D. Shaw* [1987]. Forecast error is computed for both components of the wind (u, v) . The u-component error is not only correlated with a u-component nearby, but also with a v-component error and height (z) error (by geostrophy). The correlation functions depend on latitude by similarity transformation (the spatial scale for the tropics is twice that shown here, and is 1.2 times larger in the southern hemisphere.

Table 2. Comparison of PRESCAT Winds With Experiment SCAT and NoSCAT

FGAT SCAT 930324:12, Twelve 6-hour steps							
Node	Number ($> 4\,m\,s^{-1}$)	Bias (degrees)	SD (degrees)	Number all speeds	Bias ($m\,s^{-1}$)	SD ($m\,s^{-1}$)	Vector RMS ($m\,s^{-1}$)
1	10089	–0.41	31.15	13203	–0.61	1.77	3.92
3	10109	0.42	24.49	13398	–0.59	1.72	3.30
5	10137	0.73	21.90	13560	–0.48	1.72	3.10
7	10008	1.01	20.48	13627	–0.39	1.77	3.04
9	9849	1.13	19.76	13547	–0.30	1.81	3.05
11	9722	1.47	19.10	13462	–0.26	1.83	3.04
13	9546	1.28	18.96	13291	–0.29	1.83	3.02
15	9306	1.69	18.65	12986	–0.32	1.84	3.01
17	9118	1.87	18.52	12680	–0.32	1.86	3.02
19	8963	2.37	19.62	12316	–0.33	1.85	3.03
FGAT NoSCAT 930324:12, Twelve 6-hour steps							
Node	Number ($> 4\,m\,s^{-1}$)	Bias (degrees)	SD (degrees)	Number all speeds	Bias ($m\,s^{-1}$)	SD ($m\,s^{-1}$)	Vector RMS ($m\,s^{-1}$)
1	10040	–0.89	32.14	13203	–0.64	1.88	4.06
3	10054	–0.11	25.75	13398	–0.61	1.83	3.46
5	10097	0.34	22.79	13560	–0.51	1.83	3.24
7	9971	0.80	21.47	13627	–0.42	1.87	3.19
9	9833	0.99	21.06	13547	–0.34	1.91	3.20
11	9743	1.37	20.60	13462	–0.30	1.94	3.20
13	9564	1.40	20.48	13291	–0.33	1.93	3.18
15	9310	1.70	20.08	12986	–0.36	1.93	3.17
17	9078	1.94	19.91	12680	–0.36	1.95	3.19
19	8941	2.33	20.59	12316	–0.37	1.94	3.20

For all nodes, the bias and SD of the FGAT and scatterometer wind differences and the vector RMS differences are smaller in SCAT than in NoSCAT, indicating that the SCAT FGAT has a better quality.

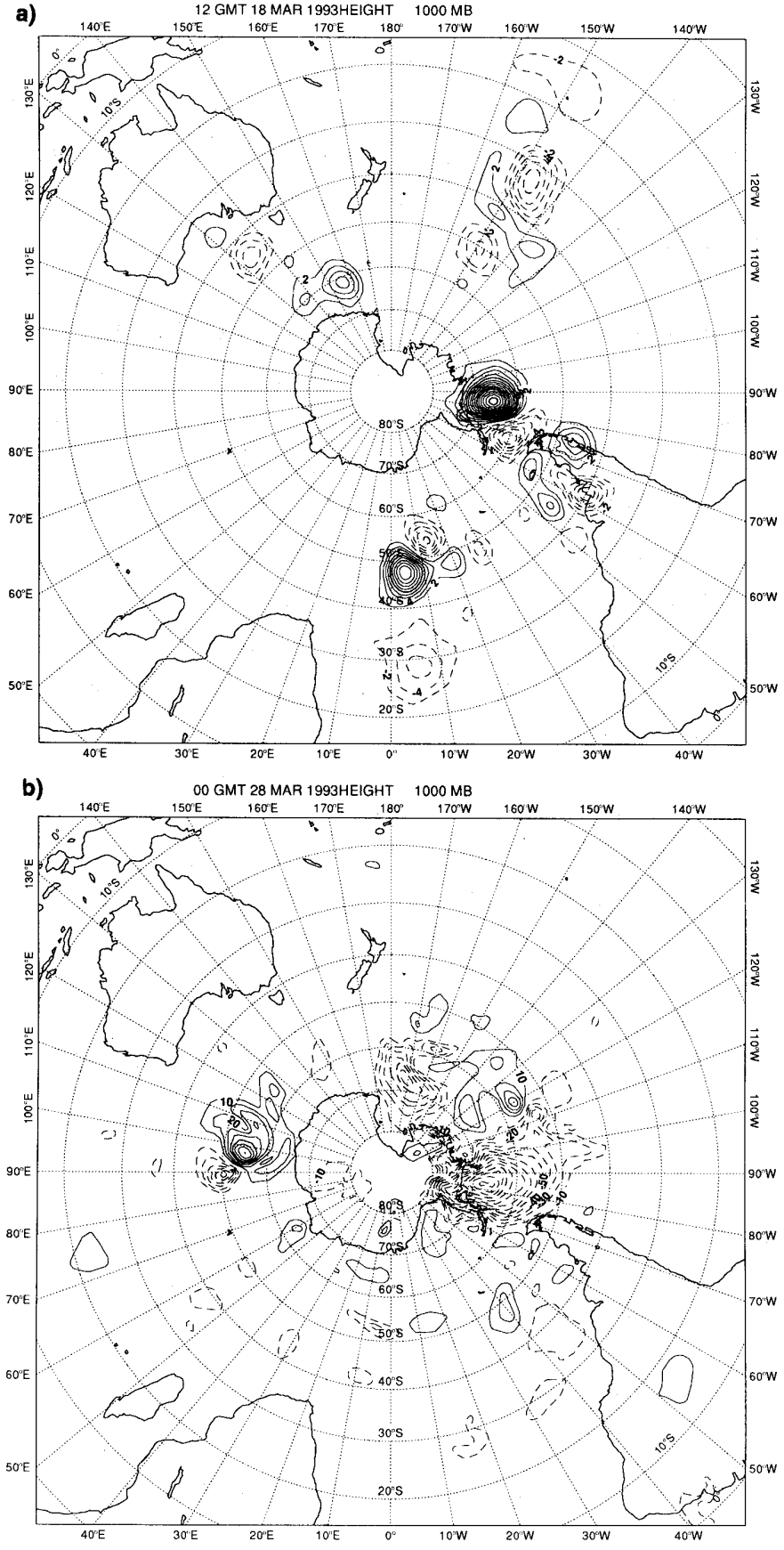

Figure 9. Differences between an analysis in which PRESCAT winds are assimilated (SCAT) and a control (NoSCAT) in which they are not used, (a) after the first assimilation, (b) after 10 days of assimilation. Field shown is the height of the 1000-hPa surface. In (a) the contour interval is 2 m; in (b) 10 m. Impact increases with time.

Table 3. The Difference Between Vector RMS Departures of SATOB and FGAT Winds for Experiments SCAT and NoSCAT

SCAT	NoSCAT
4.41 m s^{-1}	4.46 m s^{-1}

tNote the small upper air improvement by inclusion of scatterometer winds.

To verify the improvement in the upper-air first guess we made similar comparisons between SCAT and NoSCAT for SATOB winds (mainly in the subtropics and tropics), as in table 3. Again an improvement in the vector RMS departure was found, greater than 1%. The improvement was greatest in the southern hemisphere, and of similar magnitude both below and above the 700-mb level. Furthermore, we found that using FGAT from experiment SCAT in the ambiguity removal generally gave a better wind field than did FGAT from NoSCAT (one specific example is shown in Figure 4).

To be able to improve short-range forecasts is very important for severe weather prediction, and to improve forecasts of near-surface winds is useful for ocean circulation and wave models.

3.3. Medium-Range Forecast Impact

In this section, a height-anomaly-correlation skill index is used for interpretation of the impact of scatterometer data in the ECMWF analysis/forecasting system. Most of the energy in the atmosphere is in the larger spatial scales and it is to these scales that this skill index is most sensitive. The larger spatial scales are important for the medium-range forecast skill.

For the eleven days from 18 to 28 March, 10-day forecasts were made every day and compared with the corresponding operational forecasts (denoted control). All model parameters were the same in these two sets of experiments. The only differences were the analyses from which the forecasts were made: one was the control without scatterometer data (NoSCAT), and the other had assimilated scatterometer data (SCAT). Height anomaly correlations of both forecasts with the operational (i.e., NoSCAT) analyses were then calculated. Anomalies were calculated by subtracting a seasonal climatological height from the forecast and analyzed height fields before the correlation was made. An ensemble average over the 11 forecasts is given in Figure 10, which shows that assimilation of scatterometer data has had no beneficial impact on the forecasts in the sense that the anomaly correlations are, on average, the same in forecasts initiated from NoSCAT and SCAT. On the basis of forecast height anomaly correlations there is no advantage for medium-range forecasts in assimilating scatterometer data. A measure of the scatter of these forecasts is shown in Figure 11 for a forecast lead time of 72 hours. From the 11 forecasts

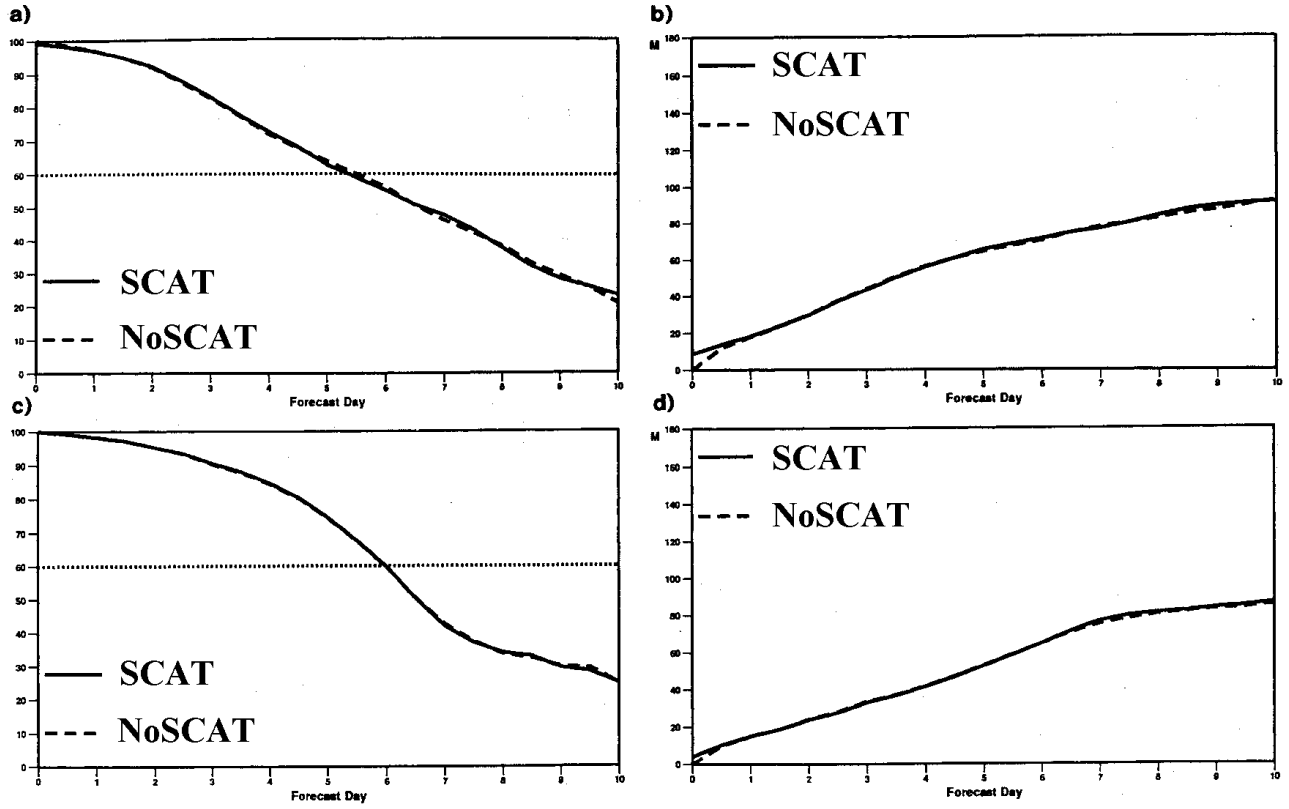

Figure 10. (a) Anomaly correlation and (b) RMS errors in the northern hemisphere for an average over the 11 forecasts initiated from SCAT and NoSCAT analyses. Similarly, (c) and (d) are for the southern hemisphere. The statistics are derived from the operational analysis (NoSCAT).

for this period, we found examples when SCAT was slightly better, not much different, or slightly worse. The differences occurred mainly in the southern hemisphere.

The neutral impact of scatterometer data in the ECMWF medium-range forecasts contrasts with the clearly beneficial impact obtained with the UK Meteorological Office's forecasting system [*Bell*, 1994]. However, by coincidence, for this particular period in March 1993 the ECMWF 5-day forecasts, without scatterometer data, had approximately 10% better RMS verifications of 500 hPa height against the ECMWF analyses than the UK Meteorological Office's forecasting system not using the data. The average improvement of 4% in the Meteorological Office 5-day forecasts when using scatterometer data is therefore insufficient to match the quality of the ECMWF 5-day forecasts. It is, therefore, harder to show a positive impact in the ECMWF system over this particular period. From statistics based on daily monitoring of forecast model quality at ECMWF we observed that the 10% difference is atypical and that, usually, the ECMWF and UKMO forecasts are closer. System and situation dependency has occurred frequently in the past in comparative studies of observation system impact.

In a second series of experiments we investigated the impact of scatterometer data in a

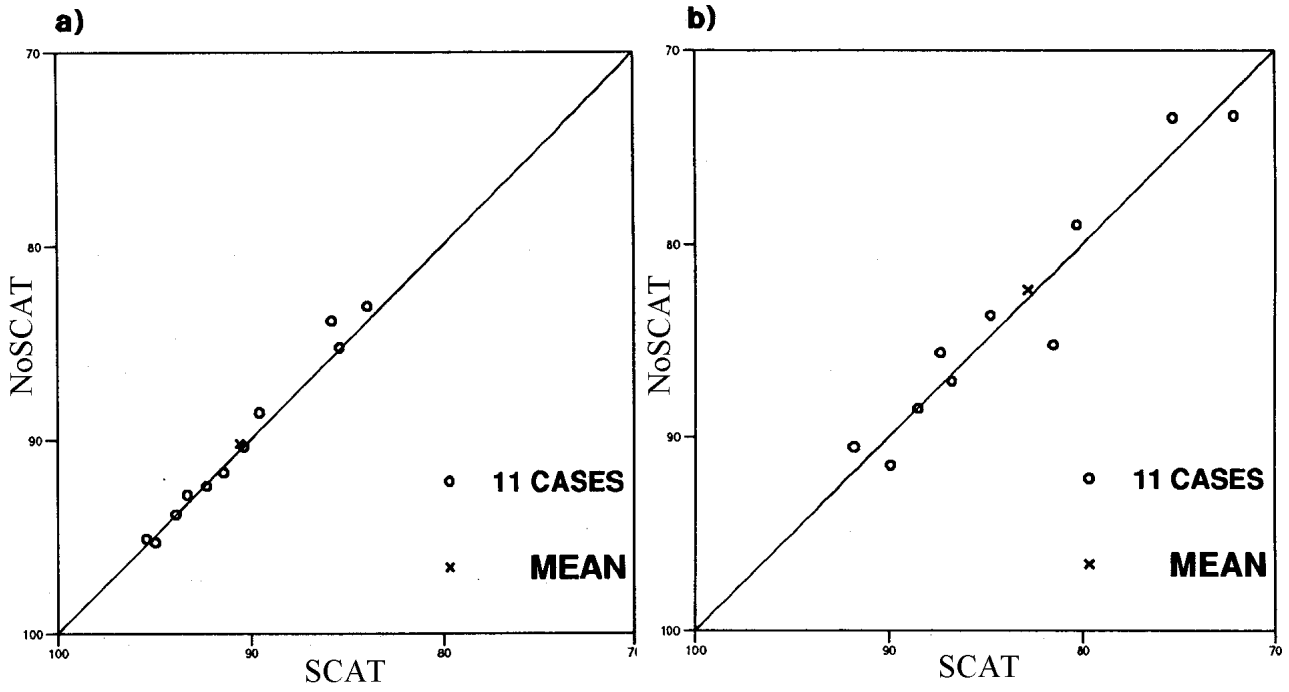

Figure 11. (a) Scatter plot of the 11 individual anomaly correlations in the northern hemisphere (20°N-90°N) for 72-hour forecasts initiated from SCAT and NoSCAT analyses. (b) As (a), but for the southern hemisphere (90°S-20°S).

degraded data assimilation system. Four separate analyses were made and from them forecast experiments were done. The first two analyses are NoSCAT/SATEM, the control without PRESCAT winds, and SCAT/SATEM which assimilated PRESCAT winds. These experiments are similar to those for March discussed above (NoSCAT and SCAT), but for a different time period. Moreover, the horizontal sampling of the model is reduced to T106 spectral truncation (125 km) and it has 19 rather than 31 levels in the vertical. Satellite temperature data, SATEMs, from the TOVS sounder [*Smith et al.*, 1979] contribute positively to the forecast scores for the southern hemisphere. SATEMs mainly define the larger scales of the analysis. SATOBs are made by tracking clouds on the imagery from geostationary satellites. They have much less impact in the southern hemisphere than have SATEMs. Two further analyses were made, removing both SATEMs and SATOBs. In one of them scatterometer winds were assimilated (SCAT/NoSAT), but not in the other (NoSCAT/NoSAT).

Average anomaly correlations in the six forecasts from these analyses, one for each day from 26 April to 1 May, are shown in Figure 12a for SCAT/SATEM and NoSCAT/SATEM, and in Figure 12b for SCAT/NoSATEM and NoSCAT/NoSATEM. Again the figures show comparisons at 1000 hPa, i.e., near the surface, but the results at 500 hPa are similar. In the case when SATEMs were used, the results are consistent with experiments SCAT and NoSCAT in that, on average, the PRESCAT winds do not lead to

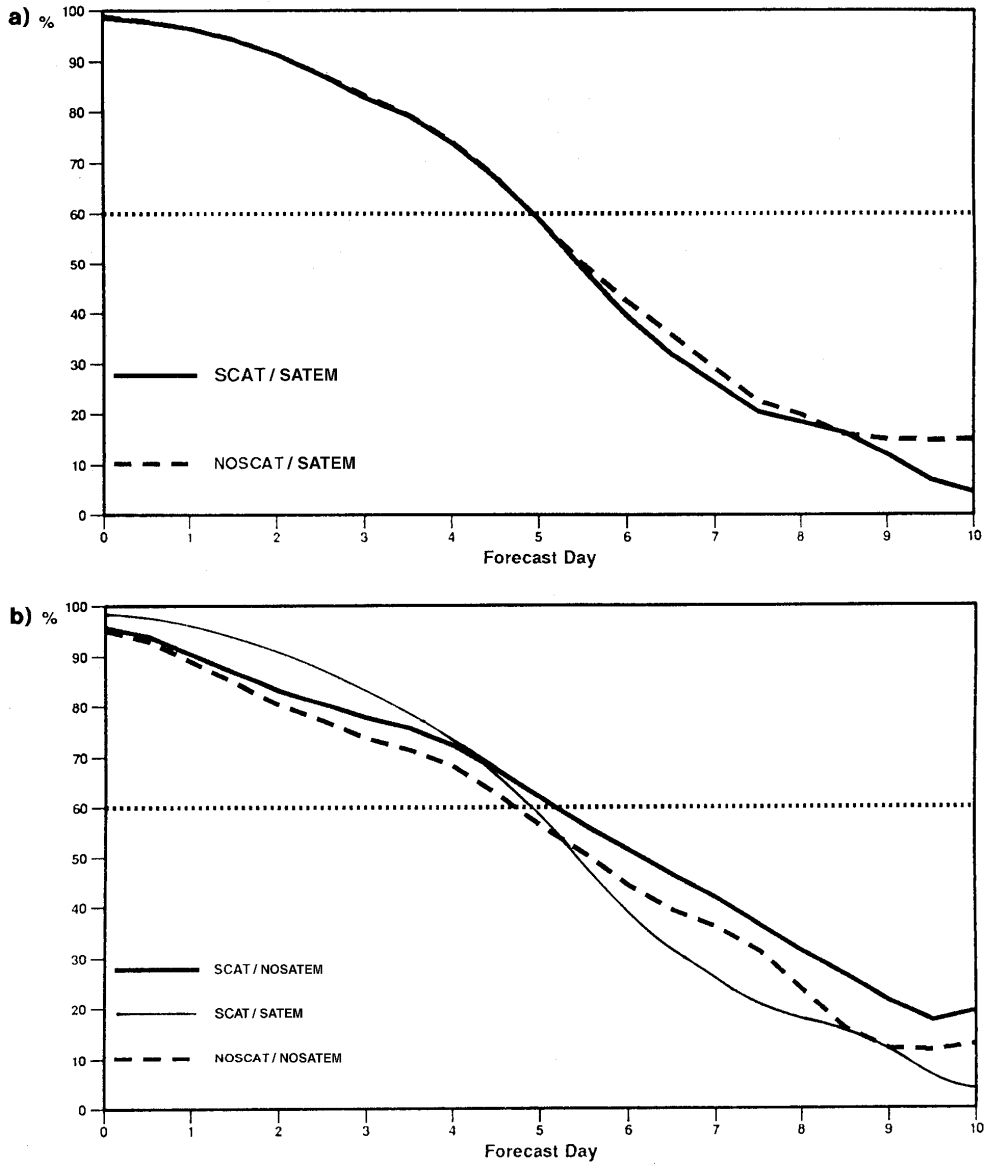

Figure 12. (a) As for Figure 10, but the averages are over the six forecasts from 26 April to 1 May, for NoSCAT/SATEM and SCAT/SATEM. The correlations are made with the operational analyses. (b) As for (a), but for experiments SCAT/NoSATEM and NoSCAT/NoSATEM. In this case, assimilation of the scatterometer winds from PRESCAT leads to improved forecasts. For comparison SCAT/SATEM is also shown.

improved forecasts. In the case when SATEMs were not used, however, the assimilation of the PRESCAT winds does lead to a significant improvement in the forecasts for the southern hemisphere. Thus, part of the lack of impact of the scatterometer in SCAT and SCAT/SATEM is because there is significant redundancy between the scatterometer and the other observing systems. If the normal observing system is degraded, for example by the removal of SATEMs (SATOBs are probably not so important), then the scatterometer will have a useful role, although, as might be expected, it will not able to compensate fully for

the loss of the thermal data provided by SATEMs throughout the atmosphere. Results similar to these have been found by *Baker et al*. [1984] and *Atlas et al*. [1985] for scatterometer data from the 1978 SEASAT mission.

3.4. Validation of the OI Data Assimilation System

When data are not used actively in the analysis they can be used to verify the analysis and subsequent forecasts, as is shown in this section for scatterometer winds. Figure 13 shows the variance of the error in the wind vector of the ECMWF model as computed over the oceans using a fixed set of scatterometer data with an estimated wind error variance of 5 $m^2 s^{-2}$. The operational ECMWF model (with no scatterometer information included) is verified at different forecast times. After the OI procedure an initialization procedure is run to filter out noise generated by OI (gravity waves). The verification of the initialized analyses (IA) and analysis (AN) are almost identical showing that the initialization filter has little effect.

The first major point to note from Figure 13 is the large increase in variance when a 6-hour forecast is interpreted as being valid at a time 2.5 hours earlier or later, compared to using a forecast at the appropriate time (FGAT). This means that using FGAT is important both for ambiguity removal (as was illustrated in section 2) and for data assimilation. If FGAT is not used for the latter, 15% of the variance of the increments will be due to a timing error and so will be incorrect. The resulting errors made in the analysis will be spatially coherent.

A second important point to note is the fact that the observations used in the analyses adversely affect the first-guess 10-m wind field over the oceans; the vector error variance of the first guess is 0.5 $m^2 s^{-2}$ (approx. 10%) lower than the vector error variance of the analyses, verified at the same locations. The average analysis minus first-guess difference (increment) over the oceans was computed to be 2.3 $m^2 s^{-2}$. So, on average a part, 0.9 $m^2 s^{-2}$ (approx. 40%), of this increment proves to be correct, and a part, 1.4 $m^2 s^{-2}$, proves wrong. In the previous section we demonstrated the positive effect of the assimilation of SATEMs and SATOBs, and scatterometer data. Here we see that the analysis increments are not necessarily beneficial in the full analysis domain, and may even be detrimental. This can be explained by the flow-independent structure functions that spread observational information in the horizontal and vertical, and project mass information on wind and vice versa (see Figures 7 and 8). As a consequence and particularly over the oceans in the southern hemisphere, the ECMWF 10-m wind analysis will be affected mainly by satellite temperature soundings. This vertical mass-to-wind projection, although valid, on average, over many cases, can be detrimental in specific cases. A case-specific and thereby flow-dependent projection would be more appropriate. However, Figure 13 also indicates that

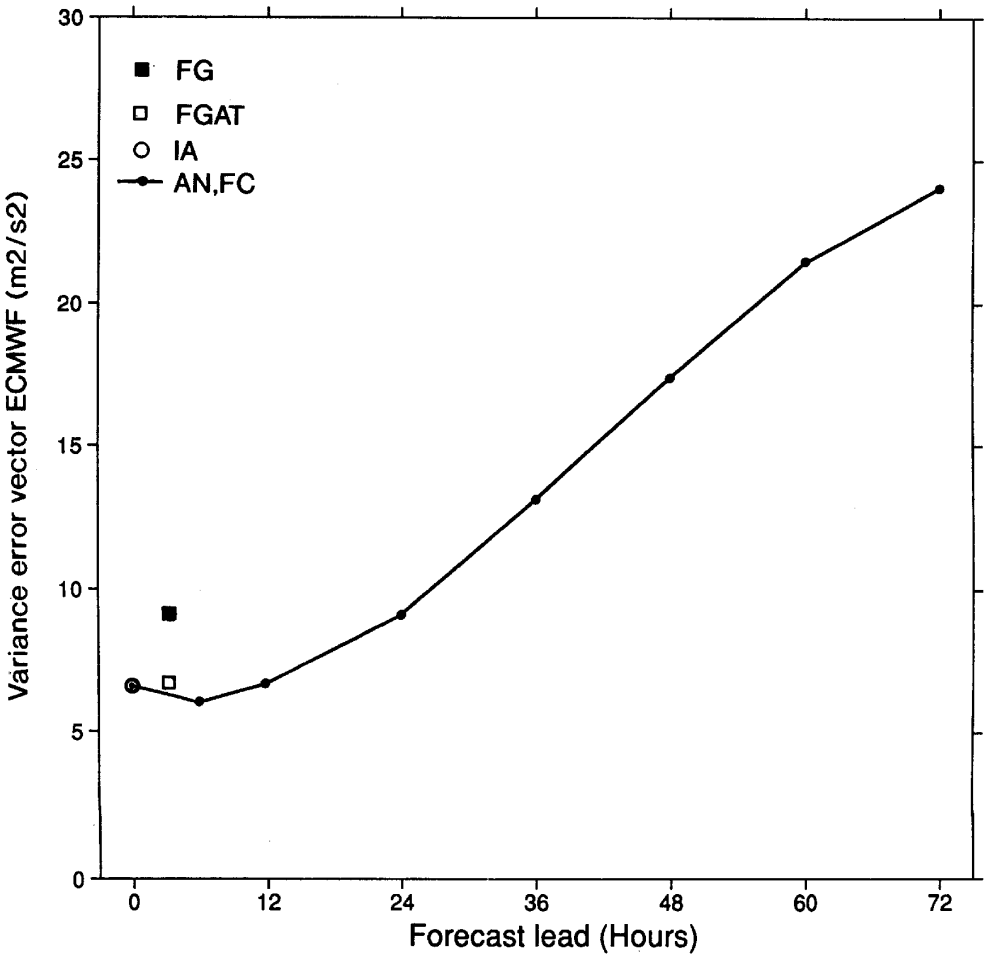

Figure 13. Wind vector error variance of the ECMWF model at a fixed set of scatterometer nodes. The wind vector error variance of the scatterometer observations was estimated to be 5 $m^2 s^{-2}$. The solid line represents from left to right the analysis, FG, and forecasts with different lead times (lead 0 corresponds to the analysis and a lead time of 6 hours to the FG). The symbol O is the initialized analysis. For this set, the time difference between scatterometer observations and the corresponding field values is less than 1 hour. The squares represent verification against another set of scatterometer winds that are between 2 and 3 hours from the FG verification time; solid squares FG and open squares FGAT.

during the 6-hour forecast the 10-m winds are again properly balanced (baroclinically) with the upper-air dynamics and become more realistic.

In section 3.3, we suggested that the analysis of scatterometer surface winds probably also adversely affects the upper-air mass field for the same reason. As a result, the mass corrections induced by the scatterometer would contradict the SATEM mass analysis-increments. Conversely, surface wind increments induced by SATEMs will contradict scatterometer wind information. It is, therefore, worthwhile that further investigation of these effects be carried out to make observational systems more complementary.

Recent studies show that in a 4D-Var system baroclinic structures can be enforced by assimilating surface (i.e., scatterometer) data [*Thépaut et al*., 1993], by using the time trajectory of the forecast model. The fact that in a 6-hour forecast the surface balance is restored, indicates that this is a promising technique which, potentially, can overcome a weakness in 3D methods.

4. Variational Methods

A variational assimilation scheme [*Le Dimet and Talagrand*, 1986] consists in the minimization of a cost function, i.e.,

$$\Im = \Im_O + \Im_B + \Im_C \tag{3}$$

where $\Im_O$ is a weighted quadratic term which measures the differences between the estimated control variables and the observations, and $\Im_B$ is a quadratic term measuring the difference between the estimated control variables and the background field. $\Im_C$ is a small term expressing physical constraints on the atmospheric state. The term $\Im_O$ describes the observation error characteristics of all observations and is the sum of the contributions of each individual observation. For each node the scatterometer penalty function, denoted $\Im_O^{SCAT}$, will be ambiguous where two penalty minima will exist corresponding to the two solutions resulting from the inversion. Furthermore, it was shown by *Stoffelen and Anderson* [1995; Chapter IV] that the total observation error of the unambiguous wind is well characterized by a normal distribution around the true wind components with a standard deviation of error of around 1.7 m s^{-1}. In this way the observation error characteristics are well defined in the wind domain. We will show in this section that the representation of the total observation error in the $\boldsymbol{s}^0$ domain is much more complex due to the highly nonlinear relationship between $\boldsymbol{s}^0$ and wind, and conclude that it is therefore more practical to define $\Im_O^{SCAT}$ in the wind domain. At the end of the section we discuss the ambiguity in $\Im_O^{SCAT}$ and show that the meteorological balance constraints incorporated in the $\Im_B$ term result implicitly in a beneficial ambiguity removal of scatterometer data in 3D-Var.

Stoffelen and Anderson [1995; Chapter II] showed that $\boldsymbol{s}^0_O$ for each node depends, essentially, on two parameters. Consequently the distribution of $\boldsymbol{s}^0_O$ triplets in the 3D measurement space is located around a 2D surface, which is cone shaped. The scatter of triplets around this cone surface is close to the instrument accuracy (5%). In the wind domain such an error corresponds to a 0.5 m s^{-1} vector RMS error, i.e., it is very small.

Following *Lorenc* [1988], we may specify the contribution of scatterometer data to the cost function in the form

$$\Im_O^{SCAT} = -2\ln\{p(\boldsymbol{s}^0_O|\boldsymbol{V})\} \tag{4}$$

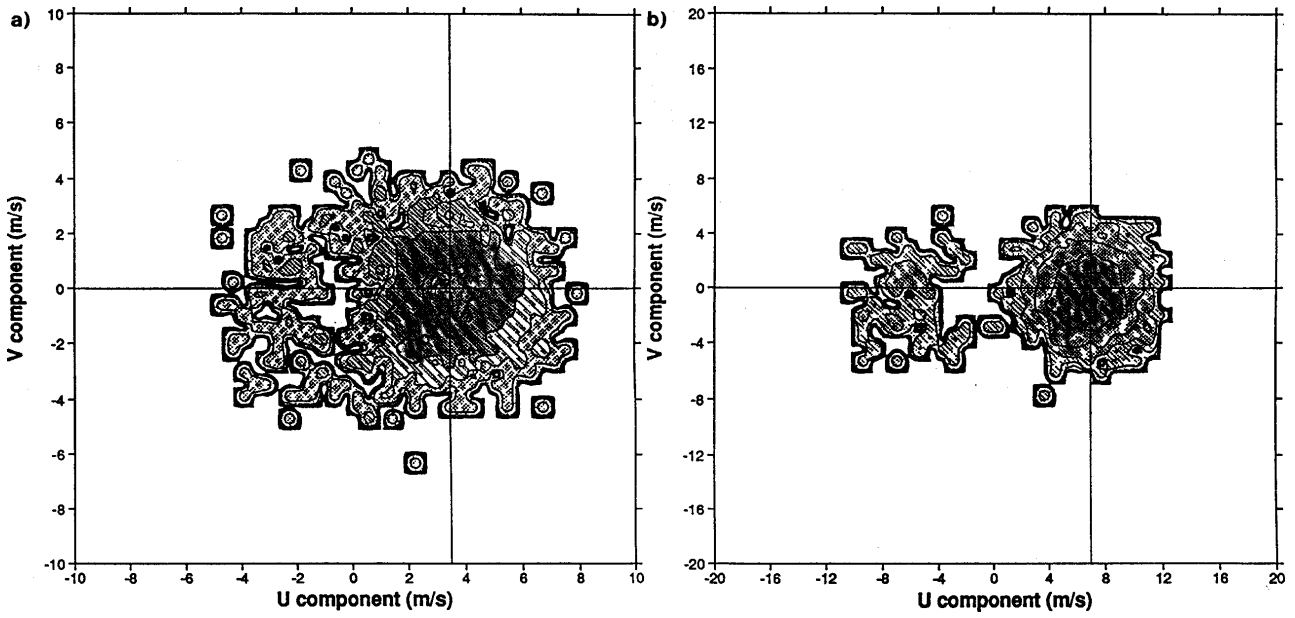

Figure 14. Monte Carlo simulations as explained in the text. The solution points are calculated with $\Im_{\mathrm{O}}^{\mathrm{SCAT}} = \Im^{\mathrm{S}}_{\mathrm{O},1}\,\Im^{\mathrm{S}}_{\mathrm{O},2}[(\Im^{\mathrm{S}}_{\mathrm{O},1})^4 + (\Im^{\mathrm{S}}_{\mathrm{O},2})^4]^{-1/4}$. In (a) the true wind speed $\boldsymbol{V}$ = (3.5, 0) in m s^{-1}, and noise e_{R} = 2 m s^{-1} and e_{B} = 2 m s^{-1}. The mean retrieved *u*-component in (a) is 3.25 m s^{-1}. Panel (b) is for $\boldsymbol{V}$ = (7, 0) m s^{-1}, and the anomalously high noise of e_{B} = 4 m s^{-1}. The mean retrieved *u* is 6.44 m s^{-1} with standard deviations of 3.29 m s^{-1} for *u* and 1.84 m s^{-1} for the *v* component. 2000 simulated scatterometer and background winds were used.

where $\boldsymbol{V}$ is the estimate for the local wind vector (control variable) and where

$$p(\boldsymbol{s}^0_{\mathrm{O}}|\boldsymbol{V}) = \int_{\boldsymbol{s}^0_{\mathrm{S}}} p(\boldsymbol{s}^0_{\mathrm{O}}|\boldsymbol{s}^0)\,p(\boldsymbol{s}^0|\boldsymbol{V})\,\mathrm{d}\boldsymbol{s}^0 \qquad (5)$$

The integral is over $\boldsymbol{s}^0_{\mathrm{S}}$, i.e., the cone as described by the transfer function, and the expression $p(a|b)$ denotes the possibility of a, given b. The first term in the integral should express the scatter observed at right angles to the cone's surface, which scatter is very small (uncertainty about the cone's location should also be included in this expression). The second term should express knowledge of the errors made when interpreting the two parameters on the surface (speed and direction), corresponding to $\boldsymbol{s}^0_{\mathrm{S}}$, as the 'true' wind vector, and of the representativeness error, i.e., the spatial and temporal scales resolved by the retrieved wind, but not resolved by the NWP model. This error constitutes the main part of the total observational error, which, in the wind domain, was easy to describe.

Now, one could attempt to assimilate $\boldsymbol{s}^0_{\mathrm{O}}$ directly into a NWP model, and project the transfer function and representativeness wind errors onto $\boldsymbol{s}^0_{\mathrm{S}}$. Because the $\boldsymbol{s}^0$ to wind relationship, as represented by the curved surface of the cone, is highly nonlinear the projection of wind errors onto the cone in the 3D measurement space is a complex problem. Certainly plane approximations using only $\partial\boldsymbol{s}^0 \setminus \partial\boldsymbol{V}$ will be inappropriate. Using the

curvature, i.e., $\partial^2 \boldsymbol{s}^0 \setminus \partial \boldsymbol{V}^2$, should be better, although still not perfect, and will certainly result in an algorithm of substantial mathematical complexity and computational cost. Moreover, in an attempt to strive for mathematical elegance, one might forget that the uncertainties regarding our knowledge of $\partial^2 \boldsymbol{s}^0 \setminus \partial \boldsymbol{V}^2$ may be a limiting factor.

Alternatively, one could try to formulate the problem in terms of wind. For this purpose, we would have to make some approximations concerning Eq. (5). As mentioned above, we can identify accurately the most likely 'true' position of a measured s^0 triplet on the cone's surface, and this inversion only results in a small contribution to the overall wind error of scatterometer winds, and so may be neglected. Therefore, replacing $p(\boldsymbol{s}^0_{\mathrm{O}} | \boldsymbol{s}^0_{\mathrm{S}})$ by $p(\boldsymbol{s}^0_{\mathrm{R}} | \boldsymbol{s}^0_{\mathrm{S}})$, with $\boldsymbol{s}^0_{\mathrm{R}}$ as derived from the inversion, we have a valid approximation. The retrieval has multiple solutions $\boldsymbol{s}^0_{\mathrm{R},i}$ because of the 180° ambiguity, and therefore the first term in the integral will be a sum of $p(\boldsymbol{s}^0_{\mathrm{R},i} | \boldsymbol{s}^0_{\mathrm{S}}) / n$, with $i = 1, ..., n$, the solution index where $n = 2$. *Stoffelen and Anderson* [1995; Chapter II] found that the two solutions have almost equal probability and therefore we have assumed no skill in the distinction of the different $\boldsymbol{s}^0_{\mathrm{R},i}$, i.e., all solutions have probability $1/n$.

The neglect of $\boldsymbol{s}^0$ measurement errors in 3D $\boldsymbol{s}^0$-space allows a further replacement of $p(\boldsymbol{s}^0_{\mathrm{R},i} | \boldsymbol{s}^0_{\mathrm{S}})$ with a Kronecker delta function of the form $d(\boldsymbol{s}^0_{\mathrm{R},i} - \boldsymbol{s}^0_{\mathrm{S}})$. After integration and using the transfer function to map $\boldsymbol{s}^0_{\mathrm{R},i}$ onto the retrieved winds $\boldsymbol{V}_{\mathrm{R},i}$, Eq. (5) reduces to

$$p(\boldsymbol{s}^0_{\mathrm{O}} | \boldsymbol{V}) = p(\boldsymbol{V}_{\mathrm{R},1} | \boldsymbol{V}) / 2 + p(\boldsymbol{V}_{\mathrm{R},2} | \boldsymbol{V}) / 2$$

As such, the formulation of the problem in wind space only needs a proper characterization of the sum of transfer-function error and the representativeness error in wind space. We may assume that

$$p(\boldsymbol{V}_{\mathrm{A}} | \boldsymbol{V}) = p(\boldsymbol{V} | \boldsymbol{V}_{\mathrm{A}}) = N(\boldsymbol{V}_{\mathrm{A}}, \boldsymbol{e}_{\mathrm{R}})$$

for an unambiguous scatterometer wind $\boldsymbol{V}_{\mathrm{A}}$, i.e., normally distributed around the components of $\boldsymbol{V}_{\mathrm{A}}$ with error $\boldsymbol{e}_{\mathrm{R}}$. Similarly, for the ambiguous solutions we may write

$$p(\boldsymbol{s}^0_{\mathrm{O}} | \boldsymbol{V}) = N(\boldsymbol{V}_{\mathrm{R},1}, \boldsymbol{e}_{\mathrm{R}}) / 2 + N(\boldsymbol{V}_{\mathrm{R},2}, \boldsymbol{e}_{\mathrm{R}}) / 2$$

From Eq. (4) we can derive the scatterometer cost function, which will not be quadratic, particularly when

$$\left\| \boldsymbol{V}_{\mathrm{R},1} - \boldsymbol{V}_{\mathrm{R},2} \right\| \leq \left\| \boldsymbol{e}_{\mathrm{R}} \right\|$$

Moreover, in these cases we find only one minimum at $\boldsymbol{V} = 0$.

An alternative analytic formulation can be found, that describes a conditional functionality in terms of the penalty function $\Im_{\mathrm{O}}^{\mathrm{SCAT}}$

$$\Im_{\mathrm{O}}^{\mathrm{SCAT}} = \left[\frac{\prod_i^2 K_i}{\sum_i^2 K_i} \right]^{\frac{1}{P}} \qquad (6)$$

where $P = 4$; $K_i = [\,\Im^{\mathrm{S}}_{\mathrm{O},i}(\boldsymbol{V}_{\mathrm{R},i})\,]^{\mathrm{P}}$, and $\Im^{\mathrm{S}}_{\mathrm{O},i}$ characterizes the estimated scatterometer wind error for one single solution, and is considered to be quadratic, as before. For low wind speeds this $\Im_{\mathrm{O}}^{\mathrm{SCAT}}$ cost function also has two minima located at $\boldsymbol{V}_{\mathrm{R},1}$ and $\boldsymbol{V}_{\mathrm{R},2}$, and a quadratic dependency on $\boldsymbol{V}$ in almost the entire speed domain, except close to $\boldsymbol{V} - \boldsymbol{V}_{\mathrm{R},1} = \boldsymbol{V} - \boldsymbol{V}_{\mathrm{R},2}$. Therefore, this formulation has more symmetry around its minima. For $P < 4$ we have a weaker gradient towards the minima, or in other words, exact ambiguity removal will be less of a constraint and intermediate solutions will be more likely. This is also the case for the cost function that was derived in the previous paragraph. From our experience with ambiguity removal we believe that a strong constraint for ambiguity removal is more appropriate; but this could be tested further.

To investigate the statistical consequence of the cost-function formulation, we performed Monte Carlo simulations. The terms $\boldsymbol{V}_{\mathrm{R},1}$ and $\boldsymbol{V}_{\mathrm{R},2}$ $(= -\boldsymbol{V}_{\mathrm{R},1})$, and a background wind $\boldsymbol{V}_{\mathrm{B}}$, we simulated for a given $\boldsymbol{V}$ using respectively a Gaussian wind-component error $\boldsymbol{e}_{\mathrm{R}}$ for the scatterometer, and $\boldsymbol{e}_{\mathrm{B}}$ for the background wind (in fact $\boldsymbol{e}_{\mathrm{B}}$ characterizes the accuracy of all available information, except the observation under investigation). Figure 14a shows a result when minimizing Eq. (3) with the above scatterometer cost function, for 2000 trials. Ambiguity removal is generally successful for a speed as low as 3.5 m s^{-1}. Figure 14b shows the distribution of solutions for 2000 simulations, but in this case $\boldsymbol{e}_{\mathrm{B}} = 4$ m s^{-1} and $V = 7$ m s^{-1}. As expected, it can be seen that ambiguity removal is less successful with reduced supporting background information. The statistical difference between the two proposed cost functions is marginal and, therefore, because of its more symmetric and quadratic behavior the functionality in Eq. (6) may be more desirable to use in a minimization. With this equation, we have arrived at a practical and accurate solution for the variational assimilation of scatterometer observations.

Preliminary results with a 3D-Var analysis system show that ambiguity removal is done accurately, and a large-scale compromise is easily found in complicated situations, as illustrated in Figure 15 (see also *Stoffelen et al* [1993]).

5. Summary and Conclusions

We have developed an ambiguity-removal scheme, called PRESCAT, as an alternative to CREO and SLICE, based on the following guidelines,

(i) that information on wind-direction retrieval skill is an important input to ambiguity removal,

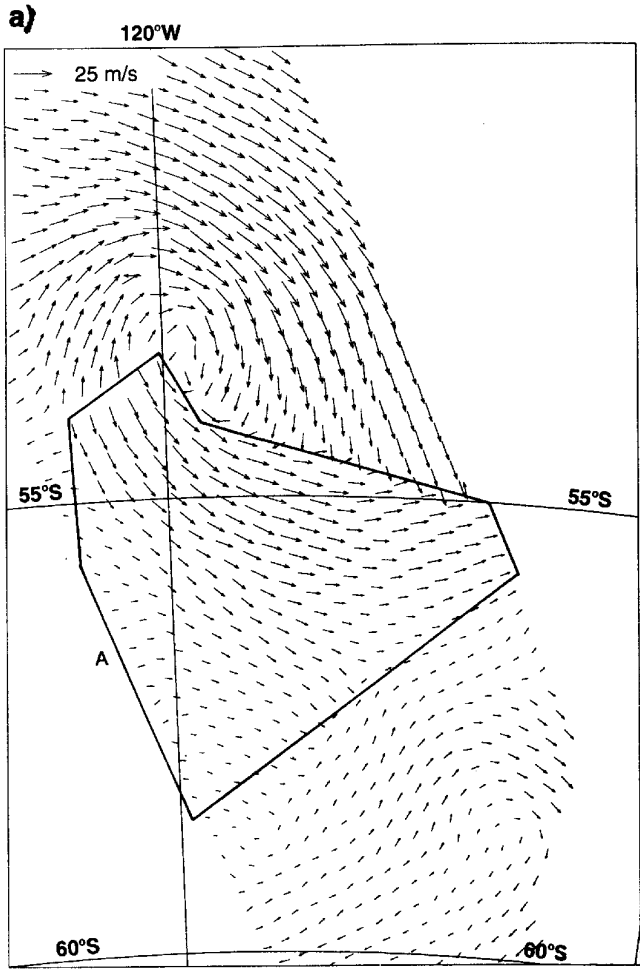

Figure 15. (a) ESA winds at 08 UTC 17 August 1993 over the south Chine Sea. On the opposing page, (b) ECMWF forecast winds, and (c) the 3D-Var analysis using information from PRESCAT and the forecast as shown in (b). The analysis in (c) illustrates, amongst other things, the ambiguity removal capability of 3D-Var.

(ii) that wind-vector filtering is beneficial compared to wind-direction filtering, and

(i) that meteorological forecast information already enables us to remove correctly about 95% of all ambiguities.

The scheme is able to remove a large percentage of the remaining ambiguities. The performance of the scheme is sensitive to the quality of the forecast wind information that we used, and we found FGAT, based on a 3-hour to 9-hour forecast, to give the best results. PRESCAT was compared with the ESA operational scheme and with SLICE for several cases and was found to be generally beneficial. The OI analysis system 'buddy' check is used effectively to identify and remove the few (approx. 0.1%) solutions wrongly selected by PRESCAT.

The PRESCAT ambiguity filter has a purely statistical nature. In meteorological analysis, physical information on the expected structure of forecast errors is also used (e.g. geostrophy). This type of information was shown to be used successfully in a 3D-Var assimilation of ambiguous winds. The development of a simple 2D method, based on the 3D-Var methodology, may be worthwhile.

Assimilation of PRESCAT scatterometer winds has a beneficial impact on the

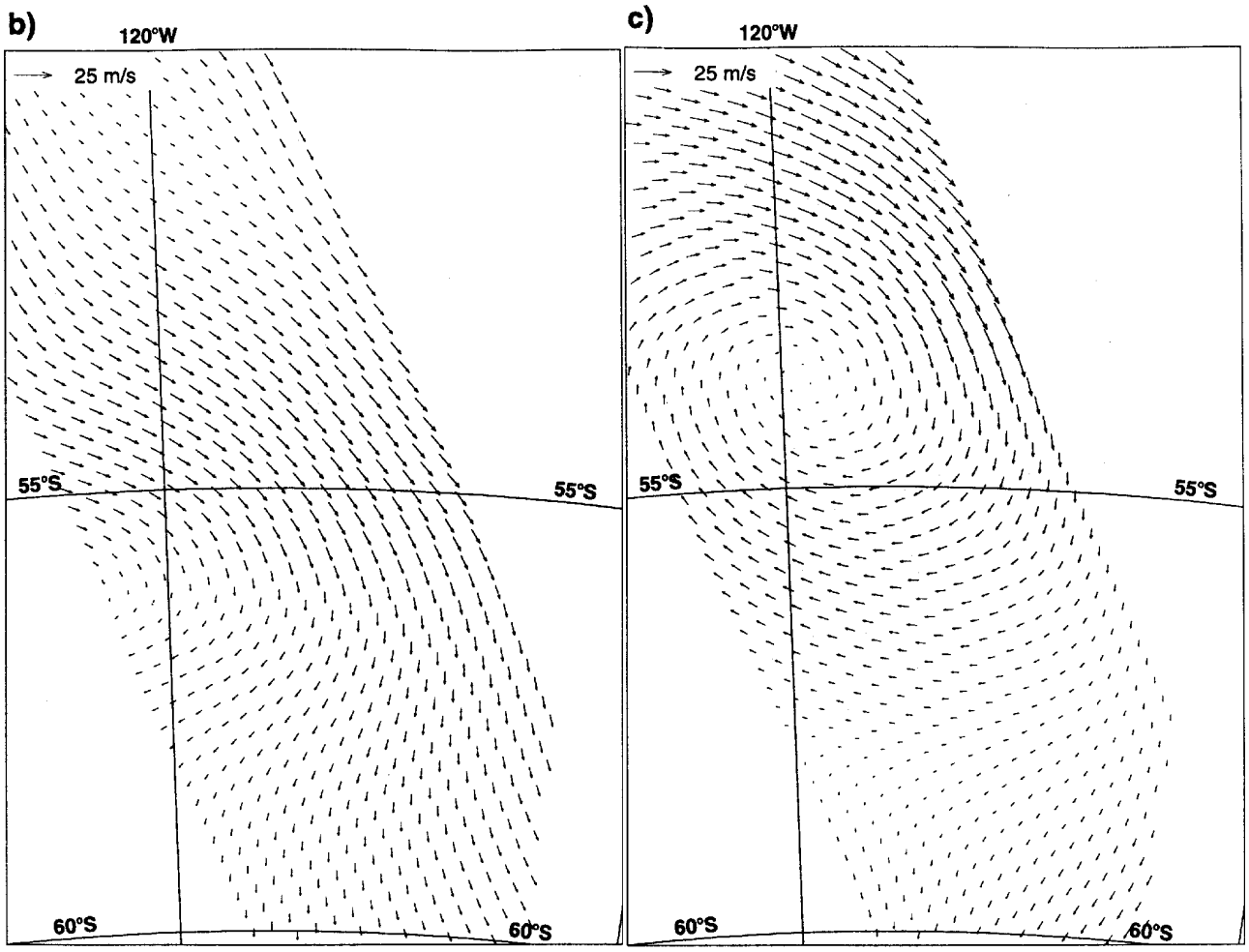

ECMWF analyses and short-range forecasts (Table 2 and 3), probably mainly from improvements at the subsynoptic scales. Ocean circulation and wave-forecast models will benefit from the improved knowledge of the winds near the surface. Also, high-resolution limited-area models, used for short-range weather forecasting, should benefit from the assimilation of scatterometer winds.

On the larger temporal and spatial scales no significant forecast impact has been found when a 'full' observing system is used. We further found that for medium-range forecasts, there is a 'redundancy' between scatterometer winds and SATEMs (satellite temperature soundings). If the latter were removed, then the scatterometer could provide beneficial large-scale information. Combining our results with the results obtained by *Bell* [1994], indicates that the impact of scatterometer data depends on assimilation system method and performance: in comparing data impact in two assimilation systems, it is more difficult to show impact in the system which is performing better for that particular period or weather regime.

Surface data are difficult to use in meteorological analysis. In most current data assimilation schemes no account is taken of the special meteorological conditions (Ekman

spiral) in the planetary boundary layer (PBL). Further, the structure functions are defined in a climatological sense and do not take into account the fact that the structure of error in the first guess will depend on meteorological conditions. The spatial structures used to update the background to fit e.g. surface observations will therefore partly be inappropriate to change the upper-air background field and, conversely, upper-air observations may have adverse effects on the surface analysis. In particular, it was shown that the global ECMWF analysis of surface wind is of a quality slightly lower than the first-guess winds, as measured by scatterometer data. When scatterometer data are used they oppose such increment structures that deteriorate the surface wind forecasts. Further investigations are needed to make the different observational systems more complementary and useful.

The above is a weakness also in 3D-Var, but in a 4D-Var assimilation scheme the sensitivity of the time trajectory of the forecast model to external forcing will mainly determine the structure of change in the model owing to an observation at a particular time and location. This will make the 4D-Var analysis meteorologically better balanced than its 3D equivalent and should lead to a more beneficial modification of upper-air fields in response to changes in the PBL.

In addition we showed that scatterometer backscatter measurements are difficult to assimilate directly, and we derived and illustrated a procedure for the assimilation of ambiguous winds.

Acknowledgments. It is a pleasure to acknowledge the constructive discussions we have had with members of the ESA analysis team and with ECMWF staff and visitors. Catherine Gaffard implemented the scatterometer processing in IFS under EUMETSAT funding. The other work was carried out at ECMWF under ESA contract 9097/90/NL/BI. Two anonymous reviewers helped by providing useful comments.

References

Anderson, D. L. T., A. Hollingsworth, S. Uppala and P. M. Woiceshyn, A study of the use of scatterometer data in the ECMWF operational analysis - forecast model Part II: Data impact, *J. Geophys. Res.*, 96, 2635-2647, 1991.

Atlas, R. , E. Kalnay and M. Halem, Impact of Satellite Temperature Sounding and Wind Data on Numerical Weather Prediction, *Optical Engineering*, 24(2), 341-346, 1985.

Baker W. E. , R. Atlas, E. Kalnay, M. Halem, P. M. Woiceshyn, Peteherych S. and D. Edelmann, Large scale analysis and forecasting experiments with wind data from SEASAT-A scatterometer, *J. Geophys Res.*, 89, 4927-4936, 1984.

Bell, R. S., Operational use of ERS-1 products in the Meteorological Office, *Proc. Second ERS-1 Symp.—Space at the Service of Our Environment, Hamburg, Germany, Eur. Space Agency Special Publ., ESA SP-361*(I), 195-200, ESA, Noordwijk, the

Netherlands, 1994.

Breivik, L.-A., Assimilation of ERS-1 scatterometer wind information in a limited area model, *DNMI Technical Report No.104*, DNMI, Oslo, Norway, 1993.

Cavanié, A. and P. Lecomte, Vol 1 - Study of a method to dealias winds from ERS-1 data. Vol 2 - Wind retrieval and dealiasing subroutines, *ESA contract 6874/87/CP-I(sc) report*, ESA publications division, Noordwijk, the Netherlands, 1987.

Courtier, P., E. Andersson, W. Heckley, G. Kelly, J. Pailleux, F. Rabier, J.-N. Thépaut, P. Undén, D. Vasiljevic, C. Cardinale, J. Eyre, M. Hamrud, J. Haseler, A. Hollingsworth, A. McNally, and A. Stoffelen, Variational assimilation at ECMWF, ECMWF *Res. Dept. Techn. Memo 194*, ECMWF, Reading, England, 1993.

Graham, R., D. Anderson, A. Hollingsworth and H. Böttger, Evaluation of ERS-1 wind extraction and ambiguity removal algorithms: meteorological and statistical evaluation, *ECMWF report*, ECMWF, Reading, England, 1989.

Hoffman, R. N., A preliminary study of the impact of C-band scatterometer wind data on global scale numerical weather prediction, *J. Geophys. Res.*, 98 (C6), 10233-10244, 1993.

Le Dimet, F-X. and O. Talagrand, Variational algorithms for analysis and assimilation of meteorological observations, *Tellus*, 38A, 97-110,1986.

Lönnberg, P. and D. Shaw, ECMWF data assimilation scientific documentation, *ECMWF Res. Manual 1, 2nd revised ed.*, ECMWF, Reading , England, 1987.

Lorenc, A. C., Optimal non-linear objective analysis, *Q. J. R. Meteorol. Soc.*, 114, 205-240, 1988.

Offiler, D., ERS-1 wind retrieval algorithms, *U. K. Meteorol. O. 19 Branch Memorandum No 86*, Meteorological Office, Bracknell, England, 1987.

Smith, W. L. , H. M. Woolf, C. M. Hayden, D. Q. Wark and L. M. McMillin, The Tiros-N operational vertical sounder, *Bul. Am. Meteorol. Soc.*, 60, 1177-1187, 1979.

Stoffelen, A. , and D. Anderson, The ECMWF contribution to the characterization, interpretation, calibration and validation of ERS-1 scatterometer backscatter measurements and their use in numerical weather prediction models', *ESA contract 9097/90/NL/BI report*, Eur. Centre for Medium-range Weather Forecasts, Reading, England, 1995.

Stoffelen, A. C. M. and G. J. Cats, The impact of SEASAT-A scatterometer data on high-resolution analyses and forecasts: The development of the QEII storm, *Mon. Wea. Rev.*, 119, 2794-2802, 1991.

Stoffelen, A. C. M., C. Gaffard and D. Anderson, ERS-1 scatterometer data assimilation, *Proc. Second ERS-1 Symp.—Space at the Service of Our Environment, Hamburg,*

Germany, Eur. Space Agency Special Publ., ESA SP-361, ESA, Noordwijk, the Netherlands, 1994.

Thépaut, J-N., R. N. Hoffman and P. Courtier, Interactions of dynamics and observations in a four-dimensional variational system, *Mon. Weather Rev.*, 121(12), 3393-3414, 1993.

Undén P., Tropical data assimilation and analyses of divergence, *Mon. Weather Rev.*, 117, 2495-2517, 1989.